1976

Higher mode dynamic plastic response of beams with finite-deflections

Soares, Carlos António Pancada Guedes

Monterey, California. Naval Postgraduate School

HIGHER MODE DYNAMIC PLASTIC RESPONSE OF BEAMS WITH FINITE-DEFLECTIONS

Carlos António Pancada Guedes Soares

HIGHER MODE DYNAMIC PLASTIC RESPONSE OF BEAMS WITH FINITE-DEFLECTIONS

by

CARLOS ANTÓNIO PANCADA GUEDES SOARES

B.S. Escola Naval, Lisboa, Portugal

(1971)

SUBMITTED IN PARTIAL FULFILLMENT OF THE REQUIREMENTS

FOR THE DEGREE OF MASTER OF SCIENCE IN CIVIL ENGINEERING

AND THE DEGREE OF OCEAN ENGINEER

at the

MASSACHUSETTS INSTITUTE OF TECHNOLOGY

May , 1976

HIGHER MODE DYNAMIC PLASTIC RESPONSE OF BEAMS WITH FINITE-DEFLECTIONS

by

CARLOS ANTÓNIO PANCADA GUEDES SOARES

Submitted to the Departments of Civil Engineering and of Ocean Engineering, on May 1976, in partial fulfillment of the requirements for the degree of Master of Science in Civil Engineering and the degree of Ocean Engineer

ABSTRACT

A study into the higher mode dynamic plastic response of beams is reported here. Within the scope of infinitesimal deflections, exact solutions are obtained for generic symmetric and antisymmetric modes, using rigid-plastic analysis. In order to account for the influence of finite deflections, an approximate procedure is used. Also a numerical procedure which satisfies the field equations at different time instants is developed. Calculations are performed for the elastic perfectly plastic case, using a finite-element formulation along with a finite-difference time integration. Results of the different solutions are compared with experiments.

Thesis Supervisor: Norman Jones

Title: Associate Professor of Ocean Engineering

Thesis Reader: José M. Roesset

Title: Professor of Civil Engineering

ACKNOWLEDGMENTS

The author is indebted to his thesis supervisor, Professor Norman Jones, for his guidance and constant advice throughout this study.

He is also indebted to Professor J.M. Roesset, Civil Engineering Department, who kindly made himself available to read the thesis.

To Professor E.A. Witmer, Department of Aeronautics and Astronautics, who, besides allowing the use of the computer program JET 3 and the blast chamber for the experiments, also provided usefull advise at different ocasions.

The experiments reported here were performed by F. Merlis and A. Abelow, and represent part of an experimental program developed by Professor Norman Jones.

The author is also thankfull to Professor M.P.Cleary, Department of Mechanical Engineering and Dr. C.T. Chon, Brown University, for their interest and helpfull discussions.

Professors J.H. Evans and R.W. Yeung, at different stages of the author stay at M.I.T. provided an invaluable advice and encouragement.

And, last but not the least, the author is deeply gratefull to his parents who provided the guidance and moral support during most of his student life and to his wife Concha who contributed significantly to his graduate studies by accepting patiently the often absent mind and providing a permanent encouragement and support which included the typing of the present work.

TABLE OF CONTENTS

LIST OF FIGURES

NOTATION

d Length of beam section covered with explosive

h_n n^{th} time step

t time

t_* $t\ V_o/H$

w Transverse displacement

v Circunferential displacement

x Axial distance

B Beam breath

D Dissipated energy in plastic work

D_i Dissipation across the i^{th} hinge

E_r Energy ratio

H Beam thickness

I Impulse

I_s Specific impulse

L Beam half-span

M Bending moment

M_o $\sigma_o H^2/4$, fully plastic moment

N Axial force

N_o $\sigma_o H$, fully plastic axial force

P Pressure

Q Transverse shear force

V Vertical force, equation (4.6)

V_o Initial impulsive velocity

W Amplitude of transverse displacement

W_* $\frac{W}{H}$

$\dot{W}_*$ $\dot{W}/V_o$

$\ddot{W}_*$ $\ddot{W}H/V_o^2$

W_e Weight of sheet explosive on a beam

W_e' Equivalent weight of explosive

W_f Final deflection amplitude

W_{*_i} Initial Velocity, equation (3.67)

W_m Maximum permanent displacement

$\dot{\alpha}_j$ Rotation rate across the j^{th} hinge

β_i Defined in equations (3.45,48,49,57,63)

γ Defined in equations (3.11,17,26,33,70,71,72)

$\bar{\gamma}$ Defined in equation (6.6)

ϵ Strain

η Location of plastic hinges

η_i Location of i^{th} plastic hinge

η_* η/L

$\dot{\eta}_*$ $H/V_o l$

$\dot{\theta}_i$ Rotation rate across the i^{th} hinge

κ Curvature change

λ Non-dimensional kinetic energy, equation (2.13)

μ Mass per unit area

ρ Density of material

σ Stress

σ_o Uniaxial yield stress

ϕ Mode shape

ϕ_i Shape of the i^{th} region of a mode

Ω_K Rotation rate across the K^{th} hinge

$(\dot{})$ $\frac{\partial}{\partial t}$ ( )

$(\ )'$ $\frac{\partial}{\partial x}$ ( )

1. INTRODUCTION

Since the work of Lee and Symonds [1] and of Conroy [2] who treated the problem of dynamic loading of rigid, perfectly plastic beams, one can identify three distint approaches that have commonly been used to solve the problems of dynamic loading of structures in the plastic range, namely: numerical treatments, generally including elastic and plastic behaviour, analytical solutions which usually neglect the elastic strains and the development of approximate procedures that predict only the overall characteristics of the dynamic response.

The numerical approach gives the possibility of analysing the detailed response of complex structures, involving both elastic and plastic behaviour (material non-linearities) and geometrical non-linearities such as large deflections. Usually these procedures can incorporate also strain hardening and strain-rate effects in the material behaviour.

The numerical schemes available are based in a special discretization of the structure and a timewise approximation of the response. Depending on the methods used for each, one can consider three basic types which use: (i) finite--differences in space and time [3,4], (ii) finite-elements in space and finite-differences in time [5,6] and (iii) fi-

nite-element discretization both in space and time [7,8].

These methods allow not only the representation of very complex structures but they also provide the time history of the transient response. They are appropriate for use in the final stages of the design of a structure, when there is enough detailed information to provide the necessary imput to these numerical procedures and, when it is required to verufy and adjust the details of the structural response.

However, in the initial phases, since there is not enough information about the structure and since one is not, in general, interested in the detailed response, simpler methods that provide a description of the overall behaviour, become more attractive.

The main simplifications involved in the analytical work consist in neglecting the elastic strains, by considering the material to be rigid for stresses smaller than a given yield stress. This approximation is valid when the kinetic energy of the disturbance is large compared with the energy that can be stored elastically in the structure. It has been shown [9,10] that the rigid perfectly plastic theory is a reasonable first order theory as long as the ratio of the mentioned energies is at least greater than three. It was also observed [10] that for energy ratios greater than about ten, elastic vibrations do not have much effect on

the results. However, the duration of dynamic loading should be short compared with the natural period of vibration of the structure. Since most of the problems of dynamic loading of structures in the plastic range are produced by blast or impact loading and are related to the desire of having the structure absorb as much energy by plastic work as possible, before fracture occurs, very often these requirements are met.

This simple rigid plastic theory has been applied to beams [11,12], frames [13], plates [14,15] and shells [16], and reasonable agreement with some experimental results [10,17,18] was obtained.

However, these solutions use a small displacement assumption, in which the equilibrium equations are enforced in the undisturbed configuration of the structure. This assumption imposes a limit on the validity of the rigid-plastic idealization, since related to high levels of energy one has large deflections. The main developments of the rigid-plastic theory consisted in considering these large deflections or geometry changes [19-21], the incorporation of strain-rate sensitivity [22-25] and strain-hardening [26,27] in the material behaviour. When these effects were included a very good agreement with experiments were observed [20,28,29].

The third line of thought, recognizes that even with

the rigid-plastic assumption, exact solutions are very difficult to obtain, except for very simple situations, because of the discontinuities involved in the material behaviour. Therefore, to avoid the direct solution of the problem, approximate procedures were developed in order to bound the final response or to approximate the deforming shape of the structure. These are respectively the Bounding and the Mode Approximation Techniques.

The basis for the bounding techniques was laid down by Martin [30] who determined a lower bound for the response time and an upper bound for the final deflection of impulsively loaded rigid-plastic structures undergoing infinitesimal deflections. Moralles and Neville [31] determined a lower bound for the final deflection and, Wierzbicki extended Martin's upper bound to the case of finite-deflections [32]. Martin [33] determined bounds for the case of time-dependent plastic behaviour and recently Symonds and Chon [34] developed an upper bound on deflection, valid for finite deflections and taking into account a time-dependent plastic behaviour.

The mode approximation techniques, as presented by Martin and Symonds [35] are based on the uniqueness proof by Martin [36] which in turn is an extension of an earlier work by Tamuzh [37].

Mode solutions were defined as being composed of two

independent functions, one of space and other of time:

$$\dot{u} = \alpha\, T(t)\, \phi\,(x) \qquad (1.1)$$

where α is a scalar. The structure is therefore reduced to a one degree of freedom system since the deformation shape remains constant while the magnitudes change with time. It was shown [35] that the time function, $T(t)$, is linear, which implies that in a mode solution the acceleration is constant. The choice of the mode shape for a given problem is not arbitrary but instead results from the minimization of the initial value of an integrated quantity that measures the difference in kinetic energy between the actual structure and the mode solution. This provides an upper bound on the error involved. This procedure, besides it's usefulness in the estimation of final deformations, provides also a better insight for the main features of the deformation process.

The mode approach first developed for time independent material behavior was extended later to rate-sensitive material [38] and to wider types of material behaviour [39].

Ho [40] extended the concept to "changing mode solutions" which are solutions without the space-time separation. This intended to account for geometry changes and for moving

or stationary discontinuity interfaces. Convergence for dynamically admissible solutions was proven. It was shown that the changing mode solution would converge to the stationary mode solutions of Martin and Symonds.

While the changing modes would correspond to the last few phases of the actual motion of the structure, the stationary mode solution was the last phase.

This extension allows a better accuracy in the predictions, especially for situations where earlier phases of motion predominate but, on the other hand, it begins loosing the simplicity of analysis which is in fact one of the major attractions of the stationary modes.

Lee [39] extended the approach, originally for impulsive loading, to include dynamic loading problems. Also elastic, viscous, rigid perfectly plastic and rigid viscoplastic behaviour were considered and it was given a wider meaning to mode solutions than just an approximation technique.

Lee defined "instantaneous mode response" of the form:

$$\ddot{u}_i(x,t) = \alpha(t)\, u_i(x,t) \qquad (1.2a)$$

$$\ddot{u}_i(x,t) = \beta(t)\, \dot{u}_i(x,t) \qquad (1.2b)$$

and used the principle of virtual work to define the instantaneous mode solution of specific problems.

He defines instantaneous elastic response as the kinematically admissible field in which the potential energy is less than in all neighboring kinematically admissible fields which possess the same total displacement. When the external loads are zero, what corresponds to the case of free-vibrations, then the motion is in a natural mode of vibration, of the form:

$$u_i(x,t) = \phi_i(x)\ T(t) \qquad (1.3)$$

as the classical normal modes of vibration.

For the rigid-plastic case, the same approach was taken and an analogy was made with the upper bound theorem of Limit Analysis [41]. Lee concluded that the true collapse load of limit analysis is the primary instantaneous mode, as defined by him.

Therefore, one could expect that the initial motion of a structure would follow the primary instantaneous mode response if the external load is arranged in such a way that it is on or slightly beyond the limit load. The implications of this fact will be discussed later in relation to Jones work [47,48].

Recently Symonds and Chon [42] extended the mode approximation technique to accomodate finite deflections.

When applying this technique to problems of finite de-

flections, because there are travelling hinges, a stationary mode solution is not applicable. Symonds and Chon considered then a sequence of instantaneous mode solutions at chosen instants of time. To go from one instant in time to the next one a numerical iterative procedure was used, so as to satisfy the field equations at that specific time instant.

Basically their mode solution satisfies all the field equations but does not necessarily satisfy the stated initial velocity condition. This corresponds to neglecting the initial phases of the motion or, the changing modes as defined by Ho.

However, good results were obtained and it was observed that the shape of the structure in sucessive mode forms changed slowly.

The authors noted that the numerical work in the application of the mode approximation, when finite-deflections are considered is much greater than in the infinitesimal case. It is however substantially less than for the exact solution. Again, when extending the technique, one faces the problem of losing the simplicity and consequently it becomes less attractive.

Recently, the bounding techniques which have been based mainly in energy considerations and the mode approximation techniques which satisfy equilibrium equations after

having a given deformation mode choosen, seem to be merging together.

One of the difficulties in the mode technique consist in the determination of a kinematically admissible displacement or velocity field.

Various procedures have been developed for a systematic determination of the approximate mode shape [35,etc] and, recently it has been shown that extremum and variational principles can be used to determine mode shapes [43,44].

Independently, Jones extended the work of Sawcsuk [45, 46] on finite deflections of plates loaded statically to the case of dynamic loading, developing an approximate procedure for beams and arbitrarily shaped non-axisymmetric plates [47] which was later extended to shells [48]. Jones' method consists on the application of the principle of virtual velocities to a kinematically admissible collapse mechanism.

The main assumption is on the choice of the applicable collapse mechanism or displacement field. Jones assumed that the shape of the displacement field due to dynamic loads is the same as the one developed for the corresponding static collapse load. It was implicit on the assumption that the profile would be the same throughout the motion or, in other words, the hinges would remain stationary, although

plastic zones are allowed to be time-dependent. The final deflection was then obtained by equating the rate of change of the initial energy to the rate of dissipation of energy by plastic work in the collapse mechanism.

Wide comparisons with experimental results have been carried out [28,29,47-51] and good agreement was obtained.

If one looks at this method in light of the so called mode approximation techniques, one realizes that it assumes a stationary mode throughout the motion. In a way, this can be considered a direct extension of the simple mode solutions of Martin and Symonds [35] to the case of finite deflections. It should be noted that Jones' method keeps the simplicity of treatment while Symonds and Chon's extension [42] is expected to give better results in the cases of significant changes of the hinge locations.

The meaning of choosing the static collapse mechanism as the kinematically admissible displacement field can be established by refering to the work of Lee [39]. This would correspond to choosing the primary instantaneous mode as being a stationary mode throughout the motion.

Recently Jones and Wierzbicki [52] studied theoretically and experimentally the higher modal dynamic plastic response of beams, associated with the determination of deformation mechanisms capable of absorbing more energy than the

first mode. They obtained an exact solution for the first three modes undergoing infinitesimal deflections and used Jones' method [47] to determine the influence of finite-deflections on the first modal response.

The present work consists of an extension of their analysis.

Within the scope of infinitesimal deflections, exact solutions are obtained for generic symmetric and antisymmetric modes. In order to account for the influence of finite deflections and to assess the relative merits of different approximate procedures, Jones' method [47] and Symonds and Chon's method [42] were applied to the first three modes. Extensions to generic symmetric and antisymmetric modes are incorporated.

Finally a comparison is done with a more compreensive elastic-plastic numerical treatment of Wu and Witmer [6] and with experimental results.

2. INFINITESIMAL DEFLECTIONS

2.1 Formulation of the problem

The present formulation basically follows the one of Jones and Wierzbicki [52].

A fully clamped beam of lenght 2L, subjected to different forms of impulsive loading, is analysed herein. It is assumed that transverse displacements are small so that strains remain infinitesimal.

Using the Bernoulli-Euler assumption of plane cross-sections remaining plane, the displacement field of the beam may be approximated by the middle plane displacements. Moreover, if transverse shear deformations and rotary inertia are neglected, the equilibrium equations for a beam subjected to an impulsive transverse loading become:

$$Q' - \mu \ddot{w} = 0 \tag{2.1a}$$

$$M' + Q = 0 \tag{2.1b}$$

where the positive sense associated with these quantities is shown in Figure 1, and the symbols are defined in Notation.

Combining both equations, one obtains the equation of motion:

$$\ddot{w} = - \frac{M''}{\mu} \tag{2.2}$$

The material is assumed rigid, perfectly plastic, neglecting therefore the effects of strain hardening and strain-rate sensitivity. The constitutive relations are then very simple, as in Figure 2. For stresses smaller than the uniaxial yield stress, σ_o, the strains are zero; at stress levels of σ_o the strains become indefinitely large, of the same sign as the stresses; stresses higher than the yield stress are not allowed:

$$\epsilon = 0 \qquad \text{if} \qquad |\sigma| < \sigma_o \tag{2.3a}$$

$$\text{sign } \epsilon = \text{sign } \sigma \qquad \text{if} \qquad |\sigma| = \sigma_o \tag{2.3b}$$

$$|\sigma| \leq \sigma_o \tag{2.3c}$$

the corresponding moment-curvature relations exibit the same behaviour [52].

To complete the formulation, boundary conditions are imposed as appropriate for each case.

The procedure followed is to postulate a kinematically admissible displacement field, introduce it in the equilibrium equations, use the constitutive relations and appropriate boundary conditions to obtain the solution. Then verify whether the solution is statically admissible. A solution that satisfies all these requirements is an "exact" solution.

In all cases considered here the velocity field is of the form

$$\dot{w}(x,t) = \phi(x)\,\dot{W}(t) \qquad (2.4)$$

where ϕ is an x-dependent function describing the shape of the mode and $\dot{W}$ is a time dependent velocity amplitude associated with the motion.

Substituting (2.4) in the equations of motion (2.2.), results in:

$$M'' = -\mu\,\ddot{W}\,\phi \qquad (2.5)$$

It should be noticed now that $\ddot{W}$ is independent of x and ϕ is independent of time. Therefore one can solve first the x-dependent part to obtain the shape and later the time--dependent to obtain the motion.

2.2 First, Second and Third Modes

These three modes have been analysed by Jones and Wierzbicki [52]. They used the time-independent acceleration fields shown in Figure 3. These acceleration fields were introduced in the equation of motion, (2.2) which was then integrated twice spacially to obtain the moment distribution. Use of the appropriate boundary conditions allowed the determination of the acceleration and location of the hinges.

The acceleration for the first mode was found to be

$$\ddot{W} = -\frac{6\,M_o}{\mu\,L^2} \qquad (2.6)$$

For the second mode it resulted

$$\ddot{W} = - \frac{6 M_o}{\mu \eta^2 L^2} \tag{2.7}$$

where

$$\eta = 2 - \sqrt{2} \tag{2.8}$$

and ηL is the location of the hinge.

It was shown that in the third mode the acceleration at the two hinges is the same and is given by (2.7), where now

$$\eta = \sqrt{2} - 1 \tag{2.9}$$

The permanent transverse displacements were obtained integrating equations (2.6) and (2.7) in time. The results for the first, second and third modes are respectively:

$$\frac{W_m}{H} = \frac{\lambda}{12} \tag{2.10}$$

$$\frac{W_m}{H} = (\sqrt{2}-1)^2 \ \frac{\lambda}{6} \tag{2.11}$$

$$\frac{W_m}{H} = (\sqrt{2}-1)^2 \ \frac{\lambda}{12} \tag{2.12}$$

where

$$\lambda = \frac{\mu V_o^2 L^2}{M_o H} = \frac{\rho V_o^2 (2L)^2}{\sigma_o H^2} \tag{2.13}$$

is a dimensionless initial kinetic energy and V_o is the peak

initial velocity at the interior hinge locations.

2.3 Symmetric Modes

Symmetric modes are defined here as the ones in which the mode shape satisfies the following:

$$\phi(x) = \phi(2L-x) \tag{2.14}$$

From an analysis of the first and third mode results [52], it is apparent that only two types of shape functions ϕ_i exist in symmetric modes.

One is applicable in the first region and is given by:

$$\text{Region 1:}\quad \phi_1 = \frac{x}{\eta_1} \qquad , \; 0 \le x \le \eta_1 \tag{2.15}$$

the corresponding boundary conditions are:

$$\text{at } x = 0 \qquad M = M_o \tag{2.16a}$$

$$\text{at } x = \eta_1 \qquad M = -M_o \tag{2.16b}$$

$$\text{at } x = \eta_1 \qquad Q = 0 \tag{2.16c}$$

Substituting (2.15) in (2.5) and using (2.16), always results in one equation of motion.

The other type of shape function is:

$$\text{Region i:}\quad \phi_i = \frac{\dot{W}_{i-1}}{\dot{W}_i}\,\frac{\eta_i - x}{\eta_i - \eta_{i-1}} - \frac{x-\eta_{i-1}}{\eta_i - \eta_{i-1}} \qquad \eta_{i-1} \le x \le \eta_i \tag{2.17}$$

where the i^{th} region has the i^{th} and i^{th}-1 hinges loca-

ted at it's extreme points η_i and η_{i-1}, and has the associated velocity amplitudes $\dot{W}_i$, $\dot{W}_{i-1}$, as indicated in Figure 4.

The applicable boundary conditions are:

$$\text{at } x = \eta_{i-1} \qquad M = \pm M_o \tag{2.18a}$$

$$\text{at } x = \eta_i \qquad M = \mp M_o \tag{2.18b}$$

$$\text{at } x = \eta_{i-1} \qquad Q = 0 \tag{2.18c}$$

$$\text{at } x = \eta_i \qquad Q = 0 \tag{2.18d}$$

Use of these conditions in conjunction with equations (2.5) and (2.17) results in one equation of motion for the i^{th} region and in the location of the $(i-1)^{th}$ hinge. It should be noted that in the last region, one has:

$$\eta_i = L \tag{2.19}$$

and therefore these are enough conditions to determine the location of all the hinges and to obtain one equation of motion for each region.

It should be noted that equations (2.15,2.16) reduce to the first mode expressions [52], when $\eta_1 = L$, and therefore we can obtain immediatly the solution for the first region from equation (2.6):

$$\ddot{W} = - \frac{6 M_o}{\mu \eta_1^2} \tag{2.20}$$

The solution for the i^{th} region, is obtained by substituting (2.17) in (2.4).

Use of (2.18) leads to

$$\ddot{W}_i = \ddot{W}_{i-1} \equiv \ddot{W} \tag{2.21}$$

$$(\eta_i - \eta_{i-1})^2 = - \frac{12\, M_o}{\mu\, \ddot{W}} \tag{2.22}$$

where $\ddot{W}$ is given by (2.20).

Introducing (2.20) in (2.22) gives the general expression for the location of the i^{th} hinge:

$$\eta_i = \eta_{i-1} + \sqrt{2}\, \eta_1 \qquad , \quad i>2 \tag{2.23}$$

Now, when we are considering the last region of each mode shape, equations (2.19) and (2.23) result in

$$L = \eta_{i-1} + \sqrt{2}\, \eta_1 \tag{2.24a}$$

and also from (2.23)

$$\eta_{i-1} = \eta_{i-2} + \sqrt{2}\, \eta_1 \tag{2.24b}$$

Equations (2.24) lead to:

$$\eta_{i-2} = L - 2\sqrt{2}\, \eta_1 \tag{2.25}$$

sucessive substitution of (2.23) in (2.25) leads to the general form:

$$\eta_o = 0.0 \tag{2.26a}$$

$$\eta_{n-i} = 1-i\sqrt{2}\ \eta_1 \quad , \quad i = 0,1,2,\ldots,n \qquad (2.26b)$$

where n is the number of interior hinges per half span of the $(2n-1)^{th}$ mode.

When $i = n-1$, (2.26b) becomes:

$$\eta_1 = \frac{L}{1+(n-1)\sqrt{2}} \qquad (2.27)$$

Substitution of (2.27) in (2.20) and (2.21) gives the general expression for the acceleration, valid in all regions:

$$\ddot{W} = -\frac{6\,M_o}{\mu\,L^2}\left[1+(n-1)\sqrt{2}\right]^2 \qquad (2.28)$$

and (2.26b) becomes:

$$\frac{\eta_i}{L} = \frac{1+(i-1)\sqrt{2}}{1+(n-1)\sqrt{2}} \quad , \quad i = 1,2,\ldots,n \qquad (2.29a)$$

$$\eta_o = 0 \qquad (2.29b)$$

It should be noticed that for $n=1$ and 2, equation (2.29) gives the previously obtained [52] hinge location for the first and third mode

2.4 Antisymmetric Modes

The antisymmetric mode shapes satisfy the following relation:

$$\phi(x) = -\phi(2L-x) \qquad (2.30)$$

In these modes there exists three types of shape functions ϕ_i. Two of them are given by equations (2.15) and (2.17) of the symmetric modes and, the third type corresponds to the region just adjacent to the midspan of the beam:

$$\phi_{n+1} = \frac{L - x}{L - \eta_n} \quad , \quad \eta_n \leq x \leq L \qquad (2.31)$$

the applicable boundary conditions are:

$$\text{at} \quad x = \eta_n \quad , \quad M = \pm M_o \qquad (2.32a)$$

$$\text{at} \quad x = L \quad , \quad M = 0 \qquad (2.32b)$$

$$\text{at} \quad x = \eta_n \quad , \quad Q = 0 \qquad (2.32c)$$

where the second condition results from antisymmetric considerations.

Introduction of (2.31) in (2.5) and satisfaction of (2.32) results in:

$$\eta_n = L - \frac{\sqrt{2}}{2}\eta_1 \qquad (2.33)$$

Introducing equation (2.23) for $i = n$ in equation (2.33) results in:

$$\eta_{n-1} = L - (\tfrac{1}{2} + 1)\sqrt{2}\,\eta_1 \qquad (2.34)$$

sucessive substitution of (2.23) in (2.34) results in:

$$\eta_{n-i} = L - (\tfrac{1}{2} + i)\sqrt{2}\,\eta_1 \qquad (2.35)$$

when $i = n-1$ this expression will give the location of the first hinge after the supports, as a function of mode number:

$$\frac{\eta_1}{L} = \frac{1}{1+\sqrt{2}\,(n-\frac{1}{2})} \qquad (2.36)$$

Introducing this in equations (2.20) and (2.35) will result in:

$$\ddot{W} = -\frac{6\,M_o}{\mu\,L^2}\,[1 + (n-\tfrac{1}{2})\sqrt{2}]^2 \qquad (2.37)$$

and

$$\eta_o = 0 \qquad (2.38a)$$

$$\frac{\eta_i}{L} = \frac{1+\sqrt{2}\,(i-1)}{1+\sqrt{2}\,(n-\frac{1}{2})} \qquad i = 1,2,\ldots n \qquad (2.38b)$$

which are the general results applicable to the $2n^{th}$ mode.

For $n = 1$ equations (2.37) and (2.38) recover the results of the second mode, equations (2.7) and (2.8) as obtained in [52].

2.5 Equations of Motion for Symmetric and Antisymmetric Modes

As resulted from the previous analysis of symmetric and antisymmetric modes, the equation of motion that governs all

the modes is the same:

$$\ddot{w} = - \frac{6 M_o}{\mu \eta_1^2} \tag{2.39}$$

where η_1 is the distance of the first hinge from the clamped end of the beam, and assumes different values, as given by equations (2.27) and (2.36).

It should be noticed that for a given mode, it results from (2.3a) that the acceleration is constant. Indeed, Martin and Symonds [35]showed that for stationary mode solutions, like the present one, the velocity varies linearly with time, which is the same as having a constant acceleration.

The initial conditions applicable to the cases considered here are, at $t = 0$,

$$w = 0 \tag{2.40a}$$

$$\dot{w} = V_o \tag{2.40b}$$

what corresponds to applying an initial velocity of triangular shape and maximum value V_o to an undeformed beam. The shape of the initial velocity imparted to the beam is equal to the corresponding mode shape as determined from the previous analysis,equations (2.15,17,31) and Reference [52].

Integrating (2.39) twice with respect to time and applying the initial conditions (2.40), results in the deflection amplitude:

$$W = V_o t - \frac{3 M_o}{\mu \eta_1^2} t^2 \tag{2.41}$$

The final deflection occurs when the velocity vanishes. This will happen at:

$$t_f = \frac{\mu V_o \eta_1^2}{6 M_o} \tag{2.42}$$

and substituting in (2.41), we will obtain the final deflection amplitude:

$$\frac{W_f}{H} = \frac{\mu V_o^2 \eta_1^2}{12 M_o} \tag{2.43a}$$

which can be rewritten as:

$$\frac{W_f}{H} = \frac{\lambda}{12} \left(\frac{\eta_1}{L}\right)^2 \tag{2.43b}$$

where λ is given by (2.13).

As the mode number increases, the corresponding value of η_1 decreases and, consequently, the final deflections decrease also.

The final deflected shape of the beam is given by:

$$\frac{W_r}{H} = \frac{\lambda}{12} \left(\frac{n_1}{L}\right)^2 \phi(x) \qquad (2.44)$$

where $\phi(x)$ is the appropriate mode shape.

For the first three modes (2.43) gives the results obtained by Jones and Wierzbicki [52].

3. APPROXIMATE PROCEDURE FOR FINITE DEFLECTIONS

3.1 Description of the Method

The approximate procedure used here is based on the theoretical study of Jones [47] mentioned previously. It consists of assuming a kinematically admissible collapse mechanism and then,by using the principle of virtual velocities, equate the energy imparted to the structure to the energy dissipated by plastic work at the hinges.

The procedure was developed for a general non axis-symmetric, initially flat, rigid perfectly plastic plate and a specialised form was presented for a plate which deforms into a number of rigid regions separated by straight line hinges.

The balance of energy for the particular case discussed above can be expressed by [47,52]:

$$\int_A (P-\mu\ddot{w})\,\dot{w}\,dA = \sum_{i=1}^{n} \int_{\ell} (Nw-M)\,\dot{\theta}_i\,d\ell \qquad (3.1)$$

where the area A on the left hand side of the equation is the total area of the plate which is subjected to the external pressure P, $\dot{\theta}_i$ is the relative angular rotation rate across the i^{th} hinge and ℓ is the length of the hinge which, in the case of the beam is it's width.

The energy dissipated per unit width of the beam is given by:

$$D = \sum_{i=1}^{n} (Nw-M)\ \dot{\theta}_i \qquad (3.2)$$

while the left hand side of (3.1) represents the work done by the external and inertia forces.

Equation (3.1) can be specialized for the case of a beam under impulsive loading by setting P=0 and performing one integration across the width of the beam, resulting in:

$$\int_x -\mu\ \ddot{w}\ \dot{w}\ dx = \sum_{i=1}^{n} (Nw-M)\ \dot{\theta}_i \qquad (3.3)$$

In the present study we will therefore apply equation (3.3) to the different modes.

The imediate consequence of dealing with finite-deflections for structures axially restrained consists on the development of membrane forces which increase in magnitude as the deflection increases, and provides a considerable reserve of strength.

In passing, it should be noted that great care should be taken when modeling structures as axially restrained since Jones showed for the static case [53] that remarkbly small in-plane displacements at the supports can change the response from that of an axially restrained beam, with considerable

reserve strengthening beyond the limit load for moderate lateral deflections, to that of a freely supported beam with no increase in strength beyond the limit load.

Neglecting the effect of transverse shear forces [54]as is appropriate at least for the lower modes [52], we must deal with the interaction curve that relates the moment and axial force.

The Johanssen yield criteria, sometimes known as the square yield curve, is known to represent well to behaviour of concrete structures [55].

The Tresca and the Mises-Hencky yield criteria represent better the behaviour of metal structures, and while the second is more accurate and more suited for numerical work [6], the Tresca yield condition being piecewise linear is in general choosen for analytical work.

However, Johanssen's yield condition is still much simpler to use than Tresca and, is has been shown [25,47,56] that even for metal structures, a square yield curve circunscribing Tresca's curve could be considered to provide a lower bound to the maximum permanent transverse displacements, while an inscribing yield curve, as shown in Figure 8, (with sides 0.618 times smaller) could be considered to give an upper bound.

Therefore, in the present study both yield conditions

will be used and the results compared.

In all cases, the assumed collapse mechanism has the same shape as the corresponding infinitesimal deflection result, and because of symmetry only half-span is analysed.

3.2 Johanssen Yield Criteria

Using this criteria, the yield condition and normality requirements will be satisfied when one has at the hinges $N = N_o$ and $M = \pm M_o$.

It should be noted that for moderate deflections, in the absence of longitudinal accelarations, equilibrium requires the axial force to be constant throughout the beam [57] and, consequently in the present case equal to N_o. In solving finite-deflection problems, very often a constant axial force is assumed [19,25,etc].

It can be shown that the left hand side of equation (3.3) for half a beam is given by:

$$\int_o^L - \mu \ddot{w} \dot{w} \, dx = - \frac{1}{3} \ddot{W} \dot{W} \qquad (3.4)$$

for all modes.

Now, for each mode, the rotation rates should be determined and introduced in (3.2) to determine the dissipated energy which, when equated to (3.4) will result in the

equations of motion.

This procedure has been used by Jones and Wierzbicki, [52] who applied it to the first mode. They obtained for the maximum deflection:

$$\frac{W_m}{H} = \frac{1}{2}\{(1+\lambda/3)^{1/2} - 1\} \qquad (3.5)$$

Here we will apply it to the modes higher than the first.

3.2.1 Second Mode

The velocity field is given by equation (2.4) where the mode shape, shown in figure 7b, is the same as for infinitesimal deflections [52]:

region 1 : $\phi_1 = \frac{x}{\eta}$ $\qquad 0 \le x \le \eta$ $\qquad (3.6a)$

region 2 : $\phi_2 = \frac{L-x}{L-\eta}$ $\qquad \eta \le x \le L$ $\qquad (3.6b)$

The corresponding rotation rates are :

at $x = 0$ $\qquad \dot{\theta} = -\frac{\dot{W}}{\eta}$ $\qquad (3.7a)$

at $x = \eta$ $\qquad \dot{\alpha} = \frac{\dot{W} L}{\eta (L-\eta)}$ $\qquad (3.7b)$

where η is given by equation (2.8), from the infinitesimal deflection analysis [52].

The normality requirements are satisfied when

at $x = 0$ $\qquad N = N_o$, $\quad M = M_o$ $\qquad (3.8a)$

at $x = \eta$ $\qquad N = N_o$, $\quad M = -M_o$ $\qquad (3.8b)$

If (3.7) and (3.8) are introduced in (3.3) we will obtain:

$$\ddot{W}_* + \gamma^2 W_* + \frac{\gamma^2}{2\sqrt{2}} = 0 \qquad (3.9)$$

where

$$\ddot{W}_* = \frac{\ddot{W}\, H}{V_o^2} \qquad (3.10a)$$

$$\dot{W}_* = \frac{\dot{W}}{V_o} \qquad (3.10b)$$

$$W_* = \frac{W}{H} \qquad (3.10c)$$

$$t_* = \frac{t\, V_o}{H} \qquad (3.10d)$$

and

$$\gamma^2 = \frac{12}{\lambda} \cdot \frac{12}{3\sqrt{2}-4} \qquad (3.11)$$

The initial conditions are, at $t_* = 0$:

$$W_* = 0 \qquad (3.12a)$$

$$\dot{W}_* = 1 \qquad (3.12b)$$

Solution of (3.9) and use of (3.12), in conjunction with the fact that the final deflection occurs when $\dot{W}_* = 0$ gives the duration of motion:

$$t_{*f} = \frac{1}{\gamma} \tan^{-1} \left(\frac{2\sqrt{2}}{\gamma}\right) \qquad (3.13)$$

and the final deflection:

$$W_{*f} = \frac{1}{2\sqrt{2}} \left\{ \left(1+\lambda \frac{6\sqrt{2}-8}{3}\right)^{1/2} - 1 \right\} \qquad (3.14)$$

Results are shown in Figure 10. When $\lambda (6\sqrt{2}-8)/3 \ll 1$ equation (3.14) reduces to the corresponding infinitesimal case result [52], equation (2.11) here.

3.2.2 Third Mode

As shown in Figure 9c, the velocity field is given by (2.4) where [52]:

$$\text{region 1:} \quad \phi_1 = \frac{x}{\eta} \quad , \quad 0 \le x \le \eta \qquad (3.14a)$$

$$\text{region 2:} \quad \phi_2 = \frac{\dot{W}_1}{\dot{W}_2} \frac{L-x}{L-\eta} - \frac{x-\eta}{L-\eta} \quad , \quad \eta \le x \le L \qquad (3.14b)$$

The rotation rates (3.7) remain valid in the present case and, in addition we have:

$$\text{at} \quad x = L \quad \dot{\Omega} = -\frac{2\dot{W}}{L-\eta} \qquad (3.15a)$$

where now, from the infinitesimal deflection [52], η is given by (2.9).

Also, in addition to the normality requirements (3.8) we have:

$$\text{at} \quad x = L \quad N = N_o \quad , \quad M = M_o \qquad (3.15b)$$

the resultant equation of motion is given by:

$$\ddot{W}_* + \gamma^2 W_* + \frac{\gamma^2}{6-2\sqrt{2}} = 0 \qquad (3.16)$$

where (3.10) remains valid and now,

$$\gamma^2 = \frac{12}{\lambda} \cdot \frac{2-3\sqrt{2}}{4-3\sqrt{2}} \qquad (3.17)$$

This equation predicts the final deflection:

$$W_{*f} = \frac{1}{6-2\sqrt{2}} \left\{ \left(1 + \frac{\lambda}{3} \frac{80-57\sqrt{2}}{2-3\sqrt{2}}\right)^{1/2} - 1 \right\} \qquad (3.18)$$

which occurs at

$$t_{*f} = \frac{1}{\gamma} \tan^{-1} \left(\frac{6-2\sqrt{2}}{\gamma}\right) \qquad (3.19)$$

Results are shown in Figure 10. When $\lambda(80-57\sqrt{2})/(6-9\sqrt{2}) \ll 1$ equation (3.19) reduces to the corresponding infinitesimal case result [52], equation (2.12) here.

3.2.3 Symmetric Modes

The collapse mechanism has the same shape as given in section 2.3. The axial force is N_o throughout and normality is satisfied having at the support $M = M_o$ and in consecutive hinges $M = \mp M_o$.

Equation (3.4) remains valid. To complete the formulation, we must now determine the dissipated energy, for a

generic i^{th} hinge, as shown in Figure 4.

The rotation rate across the i^{th} hinge, is given by:

$$\dot{\theta}_i = 2\dot{W} \frac{(\eta_{i+1} - \eta_{i-1})}{(\eta_i - \eta_{i-1})(\eta_{i+1} - \eta_i)} \tag{3.20a}$$

The location of the i^{th} hinge in the symmetric modes, is given by (2.29) and, if this is substituted in (3.20a) we obtain:

$$\dot{\theta}_i = \frac{\sqrt{2}\dot{W}}{L}[1 + \sqrt{2}(n-1)] \tag{3.20b}$$

The dissipation function corresponding to the i^{th} hinge is then given by:

$$D_i = \frac{\sqrt{2}\, M_o\, \dot{W}}{L} (1+4\frac{W}{H})[1+\sqrt{2}(n-1)] \tag{3.21}$$

where use was made of equation (3.2).

In the first region, which includes the hinge at the support and the first interior hinge, the dissipation function is given by:

$$D_1 = M_o\{1 + (1+\sqrt{2})(1+4\frac{W}{H})\}\frac{\dot{W}}{\eta_1} \tag{3.22a}$$

or, using (2.29),

$$D_1 = \frac{M_o\, \dot{W}}{L}\{1+(1+\sqrt{2})(1+4\frac{W}{H})\}[1+(n-1)\sqrt{2}] \tag{3.22b}$$

At the n^{th} hinge, which is located at x=L, the dissipa-

tion function is given by:

$$D_n = \frac{1}{2} D_i \tag{3.23}$$

since, only half of the rotation is included because only half of the beam is considered.

The total dissipation for the $(2n-1)^{th}$ mode is given by:

$$D = D_1 + (n-3/2)D_i \tag{3.24a}$$

or

$$D = \frac{M_o \dot{W}}{L} \left\{1+(1+4 \frac{W}{H}) \left[1+2\sqrt{2}(n-1)\right]\right\}\left[1+(n-1)\sqrt{2}\right] \tag{3.24b}$$

Equating (3.24) to (3.4) results in the equation of motion:

$$\ddot{W}_* + \gamma^2 W_* + \frac{\gamma^2}{2} \frac{1+\sqrt{2}\ (n-1)}{1+2\sqrt{2}\ (n-1)} = 0 \tag{3.25}$$

where

$$\gamma^2 = \frac{12}{\lambda} \left[1+2\sqrt{2}(n-1)\right] \left[1+(n-1)\sqrt{2}\right] \tag{3.26}$$

The duration of motion is given by

$$t_{*f} = \frac{1}{\gamma} \tan^{-1} \left[\frac{1}{\gamma}\left(\frac{1+\sqrt{2}\ (n-1)}{2+4\sqrt{2}(n-1)}\right)\right] \tag{3.27}$$

and the final deflection is:

$$W_{*f} = \frac{1+\sqrt{2}(n-1)}{2+4\sqrt{2}(n-1)} \left\{ \left(1+ \frac{\lambda}{3} \frac{1+2\sqrt{2}(n-1)}{\left[1+\sqrt{2}\ (n-1)\right]^3}\right)^{1/2} -1\right\} \tag{3.28}$$

For $n=1$ and $n=2$ this result reduces to equations (3.5) and (3.18) of the first [52], and third mode respectively.

3.2.4 Antisymmetric Modes

As can be observed in Figure 5, in these modes only two types of dissipation function exist. One is valid for all but the region closer to the support and the other type is valid for the first region, containing the hinge at the support and one interior hinge. It is given by:

$$D_1 = \frac{M_o \dot{W}}{L} \left[1+(1+4\,\frac{W}{H})\,\frac{2+\sqrt{2}}{2}\right]\left[1+\sqrt{2}(n-\tfrac{1}{2})\right] \qquad (3.29)$$

if use is made of equation (2.36).

The rotation rate across the i^{th} hinge is given by (3.20a). Using this equation and (2.36), one can derive the applicable dissipation function for the i^{th} hinge:

$$D_i = \frac{2\sqrt{2}\, M_o \dot{W}}{L} (1+4\,\frac{W}{H})\left[1+\sqrt{2}\,(n-\tfrac{1}{2})\right] \qquad (3.30)$$

The total dissipation for the $2n^{th}$ mode is given by:

$$D = D_1 + (n-1)\, D_i \qquad (3.31a)$$

or:

$$D = \frac{M_o \dot{W}}{L} \{\, 1+(1+4\,\frac{W}{H})\left[1+2\sqrt{2}(n-\tfrac{1}{2})\right] \}\left[1+\sqrt{2}(n-\tfrac{1}{2})\right] \qquad (3.31b)$$

Equating (3.31) to (3.4) results in the equation of motion:

$$\ddot{W}_* + \gamma^2 W_* + \frac{\gamma^2}{2} \frac{1+\sqrt{2}(n-1/2)}{1+2\sqrt{2}(n-1/2)} = 0 \qquad (3.32)$$

where

$$\gamma^2 = \frac{12}{\lambda} [1+\sqrt{2}\ (n-1/2)]\ [1+2\sqrt{2}(n-1/2)] \qquad (3.33)$$

the final deflection is given by:

$$W_{*f} = \frac{1+\sqrt{2}(n-1/2)}{2+4\sqrt{2}(n-1/2)} \left\{ \left[1+ \frac{\lambda}{3} \frac{1+2\sqrt{2}(n-1/2)}{[1+\sqrt{2}(n-1/2)]^3} \right]^{1/2} -1 \right\} \qquad (3.34)$$

and it occurs at

$$t_{*f} = \frac{1}{\gamma} \tan^{-1} \left[\frac{1}{\gamma} \frac{1+\sqrt{2}(n-1/2)}{2+4\sqrt{2}(n-1/2)} \right] \qquad (3.35)$$

When $n = 1$ these equations reduce to the second mode results, equations (3.9) to (3.13).

3.3 Tresca Yield Criteria - Moderate Deflections

In accordance with this criteria, the interaction curve between axial force and moment is parabolic, as shown in Figure 8 and can be expressed by [9]:

$$\frac{|M|}{M_o} + \frac{N^2}{N_o^2} = 1 \qquad (3.36)$$

The normality of the strain-rate vector to the yield

surface is satisfied by the associate flow rule:

$$\frac{M_o \dot{\kappa}}{N_o \dot{\epsilon}} = \frac{N_o}{2N} \quad \text{for } |N| < N_o \tag{3.37a}$$

$$-\frac{1}{2} \leq \frac{M_o \dot{\kappa}}{N_o \dot{\epsilon}} \leq \frac{1}{2} \quad \text{for } |N| = N_o \tag{3.37b}$$

where $\dot{\epsilon}$ and $\dot{\kappa}$ are the generalized plastic strain rates, the extensional strain rate and the curvature rate respectively. Using this criteria, Jones [47] derived the dissipation function for the interior hinge of a simply supported beam deforming in the first mode:

$$D_i = M_o \left(1+4 \frac{w^2}{H^2}\right) \dot{\theta}_i \tag{3.38}$$

For the case of a clamped beam, it becomes:

$$D_i = M_o \left(1+3 \frac{w^2}{H^2}\right) \dot{\theta}_i \tag{3.39}$$

Also in a clamped beam,one has for the hinge at the support:

$$D_i = M_o \left(1- \frac{w^2}{H^2}\right) \dot{\theta}_i \tag{3.40}$$

These dissipation functions are valid for $N<N_o$.

When $N = N_o$, it can be seen from equation (3.36) that the moment must vanish. When that happens, these equations are no longer applicable. It can be shown that for a clamped beam that occurs when $W_* = 1$.

The present analysis are therefore valid for deflections smaller than the beam thickness which are called here moderate deflections.

In all the cases only half of the beam is analysed because conditions of symmetry or antisymmetry apply.

3.3.1 First Mode

The velocity field is given by (2.4) where the shape is the same as used by Jones and Wierzbicki [52] for the infinitesimal case and when using the previous yield criteria. It is shown in Figure 8a and is given by:

$$\phi = \frac{x}{L} \quad , \quad 0 \leq x \leq L \tag{3.41}$$

the corresponding rotation rates are:

$$\text{at} \quad x=0 \qquad \dot{\theta} = -\frac{\dot{W}}{L} \tag{3.42a}$$

$$\text{at} \quad x=L \qquad \dot{\alpha} = \frac{2\dot{W}}{L} \tag{3.42b}$$

Using the appropriate rotation rates in conjunction with (3.39) and (3.40) and substituting all in (3.3), results in the equation of motion:

$$\ddot{W} + \frac{6\ M_o}{\mu\ L^2}\ \frac{W^2}{H^2} = -\frac{6\ M_o}{\mu\ L^2} \tag{3.43}$$

which agrees with Jones [47], when his equations of motion

are specialized for the case of impulsive loading.

This equation can be rewritten in the non-dimensional form:

$$\ddot{W}_* + \beta_1 W^2 = \beta_2 \tag{3.44}$$

where (3.8) holds and:

$$\beta_1 = \frac{6}{\lambda} \tag{3.45a}$$

$$\beta_2 = -\frac{6}{\lambda} \tag{3.45b}$$

the initial conditions to be satisfied are given by (3.12).

Solving this equation by sucessive approximations, one obtains when using the second approximation and condition (3.12):

$$W_* = t_* + \frac{\beta_2 t_*^2}{2} - \frac{\beta_1 t_*^2}{12}\left(1+ \frac{3\beta_2 t_*}{5} + \frac{\beta_2^2 t_*^2}{10}\right) \tag{3.46}$$

and

$$\dot{W}_* = 1+\beta_2 t_* - \frac{\beta_1 t_*^3}{48}\left(1+ \frac{3\beta_2 t_*}{4} + \frac{3\beta_2^2 t_*^2}{20}\right) \tag{3.47}$$

the duration of motion is obtained from equation (3.47) when satisfying the condition $\dot{W}_* = 0$. Substitution of the smallest root of the resulting equation in (3.46) will give the final deflection amplitude or, the maximum deflection.

3.3.2 Second Mode

It can be shown that for this collapse mode, described in 3.2.1, the dissipation function applicable to the interior hinges is still given by (3.39). Using this equation and (3.40), the equation of motion obtained is still (3.44) where now:

$$\beta_1 = \frac{3}{\lambda} \quad \frac{4-\sqrt{2}}{3\sqrt{2}-4} \tag{3.48a}$$

$$\beta_2 = -\frac{3}{\lambda} \quad \frac{2}{3\sqrt{2}-4} \tag{3.48b}$$

the solution for this mode is obtained from (3.46) and (3.47), using the new values of β_i .

3.3.3 Third Mode

The same velocity field of section 3.2.2 applies here. The dissipation function for the hinge at the support and the hinge next to it is, as in the second mode, given by equations (3.39) and (3.40). For the central hinge, equation (3.38) is applicable.

The equation of motion is given by (3.44) with:

$$\beta_1 = \frac{6}{\lambda} \quad \frac{6\sqrt{2}-5}{3\sqrt{2}-4} \tag{3.49a}$$

$$\beta_2 = -\frac{6}{\lambda}\ \frac{\sqrt{2}}{3\sqrt{2}-4} \qquad (3.49b)$$

the final deflection is obtained from (3.46) and (3.47). Results from all these modes are shown in Figures 8-10 compared with the solutions obtained using the previous yield criteria.

3.3.4 Symmetric Modes

The total dissipation in these modes is obtained by considering all the three types of disspation function equations (3.38-3.40). It is given by:

$$D = D_o + D_1 + (n-2)\ D_i + D_n \quad , \quad n \geq 2 \qquad (3.50a)$$

for the $(2n-1)^{th}$ mode.

For the first mode (n=1) since the central hinge is at the same time the first after the support, we have:

$$D = D_o + \frac{D_1}{2} \qquad (3.50b)$$

D_o is the dissipation function at the support and is given by:

$$D_o = \left(1-\frac{W^2}{H^2}\right)\ \frac{\dot{W}}{L}\ \left[1+\sqrt{2}(n-1)\right] \qquad (3.51)$$

where use was made of (3.40) and (2.27).

For the i^{th} hinge the rotation rate is given by (3.20b). Using this in conjunction with (3.38) and (2.27) results in

$$D_i = \left(1+4\frac{W^2}{H^2}\right)\frac{\dot{W}}{L}\,2\sqrt{2}\left[1+\sqrt{2}(n-1)\right] \tag{3.53}$$

The n^{th} hinge occurs at mid-span and the applicable dissipation for all modes except the first is given by

$$D_n = \frac{1}{2}D_i \tag{3.54}$$

Therefore, for all but the first mode, combining (3.50) to (3.54), one obtains:

$$D = \frac{M_o\dot{W}}{L}\left\{\frac{W^2}{H^2}\left[2+\sqrt{2}(8n-9)\right]+\left[2+2\sqrt{2}(n-1)\right]\right\}\left[1+\sqrt{2}(n-1)\right],\ n\geq 2 \tag{3.55}$$

Equating (3.55) to (3.4) results in

$$\ddot{W}_* + \beta_1 W_*^2 = \beta_2 \tag{3.56}$$

where

$$\beta_1 = \frac{3}{\lambda}\left[2+\sqrt{2}(8n-9)\right]\left[1+\sqrt{2}(n-1)\right] \tag{3.57a}$$

$$\beta_2 = -\frac{6}{\lambda}\left[1+\sqrt{2}(n-1)\right]^2 \tag{3.57b}$$

The solution to this equation is obtained from equations (3.46) and (3.47) using the present values of β. When $n = 3$ equations (3.57) reduce to (3.49).

3.3.5 Antisymmetric Modes

The dissipation function for the $2n^{th}$ mode is given by:

$$D = D_o + D_1 + (n-1)\, D_i \tag{3.58}$$

where now

$$D_o = \left(1 - \frac{W^2}{H^2}\right) \frac{\dot{W}}{L} \left[1+\sqrt{2}(n-1/2)\right] \tag{3.59}$$

$$D_1 = \left(1+3\,\frac{W^2}{H^2}\right) \frac{\dot{W}}{L} \left(1+\sqrt{2}\right) \left[1+\sqrt{2}(n-1/2)\right] \tag{3.60}$$

$$D_i = \left(1+4\,\frac{W^2}{H^2}\right) \frac{\dot{W}}{L}\, 2\,\sqrt{2}\, \left[1+\sqrt{2}(n-1/2)\right] \tag{3.61}$$

Combining these equations will obtain:

$$D=\frac{M_o\,\dot{W}}{L} \left\{\left[2+\sqrt{2}(8n-5)\right] \frac{W^2}{H^2} + \left[2+\sqrt{2}(2n-1)\right]\right\}\left[1+\sqrt{2}(n-1/2)\right] \tag{3.62}$$

Substituting (3.62) in (3.3) and using (3.4), will result in the equation of motion, equation (3.56), where now

$$\beta_1 = \frac{3}{\lambda} \left[2+\sqrt{2}(8n-5)\right] \left[1+\sqrt{2}(n-1/2)\right] \tag{3.63a}$$

$$\beta_2 = -\frac{3}{\lambda} \left[2+\sqrt{2}(2n-1)\right] \left[1+\sqrt{2}(n-1/2)\right] \tag{3.63b}$$

the solution of the equation of motion is given by (3.46) and (3.47).

3.4 Tresca Yield Criteria - Large Deflections

The results obtained in the previous section are valid for deflections smaller than one beam thickness. For greater deflections, the beam exibits large deflections, as defined here, in which case it behaves like a plastic string. This has been reported elsewhere [e.g. 19,47].

We will analyse here only the first three modes since it is not likely to have modes higher than these enter this range of deflections.

3.4.1 First Mode

The dissipation function applicable in this case, as given by Jones [47] is:

$$D_i = 4 M_o \frac{W}{H} \dot{\theta}_i \quad , \quad \frac{W}{H} \geq 1 \tag{3.64}$$

Equating this to (3.4), taking (3.42) into account, one obtains the equation of motion:

$$\ddot{W}_* + \gamma^2 W_* = 0 \tag{3.65}$$

where

$$\gamma^2 = \frac{12}{\lambda} \tag{3.66}$$

The initial conditions for this phase of motion are gi-

ven by equations (3.34) to (3.36), when $W_* = 1$.

The duration of first phase is given by the smallest root of the equation resulting from substituting $W_* = 1$ in equation (3.46). Substituting the resulting value of time in (3.47) will result in the initial velocity for this phase of motion, W_{*i}.

Then the initial conditions are at $t_* = t_{*i}$:

$$W_* = 1 \tag{3.67a}$$

$$\dot{W}_* = \dot{W}_{*i} \tag{3.67b}$$

Solving equation (3.65) subjected to these initial condition results in:

$$W_* = \frac{\dot{W}_{*i}}{\gamma} \sin\gamma(t_*-t_{*i}) + \cos\gamma(t_*-t_{*i}) \tag{3.68}$$

the final deflection occurs when the velocity vanishes at:

$$t_{*f} = t_{*i} + \tan^{-1}\left(\frac{\dot{W}_{*i}}{\gamma}\right) \tag{3.69}$$

and the final deflection is:

$$W_{*f} = \left(1+\frac{\dot{W}_{*i}^2}{\gamma^2}\right)^{1/2} \tag{3.70}$$

3.4.2 Second Mode

Here, equations (3.65) and (3.68) to (3.70) of the previous analysis, are still valid. However, equation (3.66) becomes now

$$\gamma^2 = \frac{12}{\lambda} \quad \frac{12}{3\sqrt{2}-4} \tag{3.71}$$

3.4.3 Third Mode

The analysis remains the same as for the previous modes except that now the different rotation rates, lead to

$$\gamma^2 = \frac{12}{\lambda} (5+3\sqrt{2}) \tag{3.72}$$

4. APPROXIMATE NUMERICAL PROCEDURE FOR FINITE DEFLECTIONS

In the case of infinitesimal deflections, considered in Reference [52] and in section 2 we were able to obtain an exact solution with a stationary mode shape because the initial velocity was arranged so as to have exactly the same shape as the mode solution and, because only bending moment was considered, consistent with the infinitesimal range of deflections. Only when these two conditions are satisfied simultaneously can an exact solution with a stationary mode be obtained.

For example, changing slightly the loading systems to be a uniform initial velocity, instead of triangular, will result in having one phase of motion in which two hinges leave the supports and travel inwards. Only when the two hinges meet together will the mode shape considered in Reference [52] or equation (3.41) prevail.

Therefore a solution only with this shape as being stationary would only approximate the motion and therefore would not be exact.

The inclusion of finite deflections in analysing cases where there are axial restrains, changes also the nature of the problem and stationary shapes can no longer be considered.

Therefore here we will consider velocity fields of the form:

$$\dot{w}(x,t) = \dot{W}(t)\ \phi(x,t) \tag{4.1}$$

where the shape of the mode is allowed to change with time.

The equilibrium equations for finite deflections are [57]:

$$M'' - (N w')' + \mu \ddot{w} = 0 \tag{4.2a}$$

$$Q = - M' \tag{4.2b}$$

$$N' = 0 \tag{4.2c}$$

in the absence of transverse and longitudinal pressure loading. From (4.2a) and (4.2c), it results:

$$M'' - N w'' + \mu \ddot{w} = 0 \tag{4.3}$$

It is apparent from section 3 that the consideration of the Johanssen or of Tresca yield condition do not change the general concepts involved and that in general Johanssen's relation leads to less complicated treatments. Therefore, in this section, only the square interaction curve will be used to obtain the results.

4.1 First Mode

As now we will allow the mode to change with time, we

will not restrict the interior hinge to be located at center of the beam. Therefore, we will formulate the problem for the entire beam, of length 2L, while in the previous analysis only half span was considered.

We will however be restricting the solution in that we will not account for situations such as two hinges spreading from the center of the beam, leaving a rigid region between or, any other mode form, except the one which has only one hinge in the interior of the beam.

The mode shape is then given by:

$$\text{region 1: } \phi_1(x,t) = \frac{x}{\eta} \qquad 0 \le x \le \eta \qquad (4.4a)$$

$$\text{region 2: } \phi_2(x,t) = \frac{2L-x}{2L-\eta} \qquad \eta \le x \le 2L \qquad (4.4b)$$

where now η varies with time and its time derivatives must be considered. It should be noted that this mode shape is not a symmetric one and is therefore applicable to any triangular initial velocity condition, with it's peak at $x=\eta$.

Equation (4.2c) together with the yield criteria imposes that $N = N_o$ throughout.

The applicable boundary conditions are:

$$\text{at } x = 0 \qquad M = M_o \qquad (4.5a)$$

$$\text{at } x = \eta \qquad M = -M_o \qquad (4.5b)$$

$$\text{at } x = 2L \qquad M = M_o$$

at $x = \eta$ $\quad V = 0$ (4.5d)

where V is defined as the vertical force and is given by:

$$V = Q + N_o w' \tag{4.6}$$

Introducing now (4.1) and (4.4a) in (4.3) and using conditions (4.5a,b,d) results in:

$$\ddot{W} - \frac{\dot{\eta}\dot{W}}{\eta} - + \frac{3 N_o}{\mu \eta^2} W + \frac{6 M_o}{\mu \eta^2} = 0 \tag{4.7}$$

Use of (4.4b) and (4.5b-d) in the equilibrium equation, (4.3) results in:

$$\ddot{W} - \frac{\dot{W}\dot{\eta}}{2L-\eta} + \frac{3 N_o}{\mu(2L-\eta)^2} + \frac{6 M_o}{\mu(2L-\eta)^2} = 0 \tag{4.8}$$

If one now introduces $\ddot{W}$ from equation (4.8) in (4.7), the result is:

$$\dot{\eta} = \frac{(L-\eta)^2}{2L-\eta} \frac{6 M_o}{\mu \dot{W} \eta L} \left(1+2 \frac{W}{H}\right) \tag{4.9}$$

this equation gives the velocity of propagation of the hinge. It should be noted that it vanishes when $\eta = L$.

The applied velocity field is symmetric and has it's maximum value at $x=L$. Then, the initial conditions are at $t = 0$:

$$\eta = L \tag{4.10a}$$

$$W = 0 \tag{4.10b}$$

$$\dot{W} = V_o \tag{4.10c}$$

Therefore the hinge is initially at $\eta = L$ and the velocity of it's propagation clearly vanishes. In this case we have therefore a stationary hinge as given by this formulation.

Therefore equations (4.7) and (4.8) reduce just to

$$\ddot{W} + \frac{3\,N_o}{\mu\,L^2} W + \frac{6\,M_o}{\mu L^2} = 0 \tag{4.11a}$$

It's non-dimensional form is simply:

$$\ddot{W}_* + \frac{12}{\lambda}\ W_* + \frac{6}{\lambda} = 0 \tag{4.11b}$$

It should be noted that because of the stationarity of the hinge, this solution reduces to the case considered by Jones and Wierzbicki [52] when taking finite deflections into account.

Also, the stationarity of the hinge is the result of the symmetry of the initial velocity. The formulation, equations (4.8) and (4.9) handles the more general case of non-symmetric initial conditions, in which case equation (4.9) predicts a moving hinge.

4.2 Second Mode

The velocity field is given in this case by (4.1) and (3.6) where in the last one η varies with time. The boundary conditions are given by:

$$\text{at} \quad x = 0 \qquad M = M_o \tag{4.12a}$$

$$\text{at} \quad x = \eta \qquad M = -M_o \tag{4.12b}$$

$$\text{at} \quad x = L \qquad M = 0 \tag{4.12c}$$

$$\text{at} \quad x = \eta \qquad V = 0 \tag{4.12d}$$

where (4.12c) results from antisymmetry and V is given by (4.6).

Introducing the velocity field corresponding to the first region in the equilibrium equations, (4.3) and using the appropriate boundary conditions results in:

$$\ddot{W} - \frac{\dot{\eta}}{\eta}\dot{W} + \frac{3\,N_o}{\mu\,\eta^2}\,W + \frac{6\,M_o}{\mu\,\eta^2} = 0 \tag{4.13}$$

Performing the same for the second region, results in:

$$\ddot{W} + \dot{W}\,\frac{\dot{\eta}}{L-\eta} + \frac{3\,N_o}{\mu(L-\eta)^2}\,W + \frac{3\,M_o}{\mu(L-\eta)^2} = 0 \tag{4.14}$$

Now we must solve these two equations for the deflection W and for the hinge location η. In non-dimensional form they will be respectively:

$$\dot{\eta}_* = \frac{6}{\lambda \eta_* W_*} + \frac{12\, W_*}{\lambda\, \eta_* W_*} + \frac{\eta_*\, \ddot{W}_*}{W_*} \tag{4.15}$$

$$\ddot{W}_* = -\frac{3(2-\eta_*)}{\lambda\, \eta_*(1-\eta_*)} - \frac{12\, W_*}{\lambda\, \eta_*(1-\eta_*)} \tag{4.16}$$

where

$$\eta_* = \frac{\eta}{L} \tag{4.17a}$$

$$\dot{\eta}_* = \frac{\dot{\eta}\, H}{V_o\, L} \tag{4.17b}$$

These equations will be solved numerically, as indicated later.

4.3 Third Mode

The velocity field is given by (4.1) and (3.14) where η is to be understood as time varying. The applicable boundary conditions are:

$$\text{at} \quad x = 0 \qquad M = M_o \tag{4.18a}$$

$$\text{at} \quad x = \eta \qquad M = -M_o \tag{4.18b}$$

$$\text{at} \quad x = L \qquad M = M_o \tag{4.18c}$$

$$\text{at} \quad x = \eta \qquad V = 0 \tag{4.18d}$$

$$\text{at} \quad x = L \qquad V = 0 \tag{4.18e}$$

Introduction of the velocity field (3.14) in the equilibrium equations, (4.3), and use of conditions (4.18a-c) leads to the expressions of moment in the two regions. Use of conditions (4.18d,e) will result in the equations of motion, which can be written as:

$$\ddot{W}_{*1} = \frac{8}{\lambda \eta_* (1-\eta_*)^2} \left[W_{*o} (1-3\eta_*) - 2\eta_* W_{*1} \right] - \frac{6}{\lambda (1-\eta_*)^2} \qquad (4.19)$$

$$\ddot{W}_{*o} = \frac{8}{\lambda \eta_*} \frac{W_{*o} + W_{*1} \eta_*}{(1-\eta_*)^2} - (\dot{W}_{*o} + \dot{W}_{*1}) \frac{\dot{\eta}_*}{1-\eta_*} + \ddot{W}_{*1} \qquad (4.20)$$

$$\dot{\eta}_* = \frac{\ddot{W}_{*o} \eta_*}{\dot{W}_{*o}} + \frac{12 W_{*o}}{\lambda \dot{W}_{*o} \eta_*} + \frac{6}{\lambda \dot{W}_{*o} \eta_*} \qquad (4.21)$$

where now the velocities in the central region $\dot{W}_1$ and on the lateral regions $\dot{W}_o$ are no longer equal.

These equations will be solved numerically.

4.4 Numerical Timewise Solution

While for the infinitesimal case it was possible to obtain an analytical solution of the equations of motion, now we will solve them numerically since they don't seem amenable to a closed form solution.

There exists a wide range of integration operators

that have been used sucessfully in structural dynamic problems [58]. Their characteristics as to stability, converge and damping are well known [59], except for the recent and apparently more attractive Park's method [60,61].

Because in the present problem the elastic vibrations are neglected no major stability problems are expected and, instead of the more sofisticated operators such as Park and Houbolt , a Newmark β operator [62]will be used.

The Newmark β operator, for $\gamma = 1/2$ and $\beta = 1/4$, also known as the trapezoidal method or the average acceleration method [63], exibits very good characteristics for linear problems, such as being unconditionally stable ($\beta = 1/4$) and introducing no false damping ($\gamma = 1/2$).

However, for non-linear problems, stability is not assured.

The average acceleration method is an implicit method in that it needs information about the time step to be calculated, before it calculates it. Basically it uses for the value of acceleration during one time step the average value of the accelerations at its begining and end. Therefore, if no extrapolation scheme is used, as was choosen here, iteration becomes necessary.

In general, for the n^{th} time step, the values of the

velocities and deflections are given by:

$$\dot{W}_n = \dot{W}_{n-1} + \frac{h_n}{2} (\ddot{W}_n + \ddot{W}_{n-1}) \tag{4.22a}$$

$$W_n = W_n + \frac{h_n}{2} (\dot{W}_n + \dot{W}_{n-1}) \tag{4.22b}$$

where h_n is the n^{th} time step.

For the present equations, one is dealing also with the hinge location. Considering the integration of this quantity and rewritting the equations (4.22) in a form more suitable to iteration, one has:

$$\dot{W}_n = A_{n-1} + \frac{1}{2} \ddot{W}_n \, h_n \tag{4.23}$$

$$W_n = B_{n-1} + \frac{1}{2} \dot{W}_n \, h_n \tag{4.24}$$

$$\eta_n = C_{n-1} + \frac{1}{2} \dot{\eta}_n \, h_n \tag{4.25}$$

where

$$A_{n-1} = \dot{W}_{n-1} + \frac{1}{2} \ddot{W}_{n-1} \, h_n \tag{4.26a}$$

$$B_{n-1} = W_{n-1} + \frac{1}{2} \dot{W}_{n-1} \, h_n \tag{4.26b}$$

$$C_{n-1} = \eta_{n-1} + \frac{1}{2} \dot{\eta}_{n-1} \, h_n \tag{4.26c}$$

the values of the acceleration W_n and hinge velocity η_n are obtained from the equations of motion.

For the first mode, the hinge velocity was always zero and there is only one equation to be solved, (4.11), which turns out to have closed form solution [52]. However, it was also integrated numerically to verify the accuracy of the numerical calculations and, a perfect agreement was achieved.

For the second mode we have to solve equations (4.15) and (4.16). The procedure used in this case was as follows: to obtain the values at time step $t_n = \sum_{t=1}^{n} h_i$ begin by determining the constants (4.26) which will remain unchanged during the iterations in the given time step; next assume that $\ddot{W}_n = \ddot{W}_{n-1}$ and $\dot{\eta}_n = \dot{\eta}_{n-1}$ and determine (4.23) to (4.25); substitute the calculated values sucessively in (4.16) and in (4.15) to obtain W_n and $\dot{\eta}_n$; if these values differ from the initially assumed values by differences greater than the established convergence criteria, repeat the process until satisfactory convergence is attained; when the solution converged can go to next time step. The solution is considered to have converged when it agrees in the fourth decimal place. The procedure for the second mode is started by the initial conditions:

$$W_1 = 0 \qquad (4.27)$$

$$\dot{W}_1 = 1 \qquad (4.27b)$$

$$\eta_1 = 2 - \sqrt{2} \qquad (4.27c)$$

The initial value of acceleration and hinge velocity is obtained by substituting (4.27) in (4.16) and (4.15).

For the third mode three equations need to be solved, for W_o, W_1, and η , (4.18-20). The general procedure is the same as for the second mode except that now at each time step we need to achieve convergence in three variables instead of only two.

In Figures 11 and 12 it is shown the time variation of all these variables for the first and second modes for a value of $\lambda = 50$. It should be noted that the equations solved were in non-dimensional form and the results are applicable to the non-dimensional variables as defined before.

Appendix contains a listing of the computer programs used to perform these computations.

Calculations were made for different values of λ so as to determine the variation of final deflection with λ and these results are compared in Figures 8 and 9 with the previous solutions and with the experimental results.

5. ELASTIC-PLASTIC NUMERICAL APPROACH

The calculations made for the elastic-plastic behaviour of the beams, utilized the computer program JET 3, developed by Wu and Witmer [64].

The program, originally developed to calculate large elastic plastic dynamically induced deformations of free and restrained, partial and / or complete structural rings, can be used to analyse beams since it handles rings of arbitrary curvature.

The program is based on the theoretical development reported in [6]. It uses the assumed displacement version of the finite-element method to model the structure, together with the temporal finite-difference approximation. The equations of motion for the spatial finite-element formulation are derived from the Principle of Virtual Work and D'Alembert's Principle. The Mises-Hencky yield criteria and it's associated flow rule are adopted to describe the elastic plastic behaviour of the material. The strain-hardening behaviour is taken into account by using the mechanical sublayer material model. The strain-rate effect is approximated by assuming that the uniaxial stress-strain relation is affected the strain rate only by a quasi-steady increase in the yield stress above the static-test yield stress. The

program incorporates the Bernoulli-Euler (or Kirchoff) hypothesis, excluding transverse shear deformation.

The behaviour of each finite-element is characterized by four generalized displacements at each node:

$$v, w, \quad \psi = \frac{\partial w}{\partial \eta} - \frac{v}{R} \quad \text{and} \quad \chi = \frac{\partial v}{\partial \eta} + \frac{w}{R}$$

where v and w are mid-plane displacements in the circunferential and normal direction, R the radius of curvature and η the length cordinate. The displacement behaviour is represented by a cubic polynominal in η for both the circunferential, v , and the normal displacement w.

Besides elastic restrains JET 3 includes three types of nodal displacement conditions namely, symmetry ($v = \psi = 0$), ideally clamped ($v = w = \psi = 0$) and smoothly-hinged ($v = w = 0$).

As forcing function, the program accepts initial velocities and transient externally applied loads. These can be described as concentrated at the nodes, uniformly distributed or with a sine shape over the elements.

The equations of motion are solved by applying an appropriate timewise finite-difference operator which provides a solution step-by-step in finite-time increments. Two options are available for the integration operator: (1) the explicit

3-point central difference operator and (2) the implicit Houbolt operator which uses a 4-point backward difference.

The program is subdivided in four subprograms JET 3A to JET 3D which handle four different groups of problems.

For the present calculations, it was choosen to use the Houbolt operator, since it allows the use of larger time steps and we are interested in the final deflection of the beams analysed.

However, while for the central difference operator there exists a stability criterion for linear dynamic systems, which allow the estimation of the appropriate Δt to be used, no such criteria exists for the Houbolt operator and the choice of Δt must be based on numerical experimentation.

Based on the numerical calculations reported in [6] for an impulsively loaded beam, it seemed appropriate to choose a Δt of 5μsec.

While for the central difference method unstable solution show unreasonably large deflections, for the Houbolt operator a gradual degradation of the response may occur for large-deflection, non-linear response problems. Therefore, initially a calculation was performed also using Δt= =3μsec to assure that a Δt of 5μsec was providing the converged solution. This was done for specimen 9 of ref.

[52] which deforms in the second mode and identical results within plotting accuracy were obtained, as shown in Figure 14. The rest of the calculations were performed using a Δt of $5\mu sec$.

Because of antisymmetry considerations only half of the beam was analysed and 10 elements of equal length were used. The boundary conditions used were fully clamped at the support and smoothly hinged at midspan.

Basically the information the program needs consists of the mode locations and the shape of the prescribed initial velocity. The initial velocity was given by it's value and slope at the nodal stations. As a result, the vicinity of the peak velocity was approximated by a higher order curve, resulting in higher velocities being introduced. The kinetic energy that was given to the program resulted 2% higher that in the experiment.

However, this would correspond to a higher velocity and a higher value of λ. In Figure 8 the final deflection is shown, corrected for new value of λ, and Figure 14 contains the full time history of the response.

The final deflection is estimated by an average between it's maximum and minimum values after some vibratory cycles have elapsed.

The same calculations were performed for specimen 10 of Reference [52]. Now 19 elements of different size were used. A smaller one was centered at the peak velocity location and in it's vicinity finer mesh was used. The same type of result was obtained, as can be seen in Figures 8 and 15.

6. EXPERIMENTAL DETAILS

The general experimental arrangement used was similar to that employed by Jones in several previous studies [28, 29,49,50,52].

The present experiments represent a continuation of the studies reported in [52]. A reader is refered to it for a more complete discussion of the experimental details.

The tests reported here were conducted on fully clamped beams made of aluminum 6061 T6511 ($E = 10.5 \times 10^6$ lb/in^2, $\rho = 0.000251$ lb.sec^2/in^4). The beams were nominally 5 in long 0.6 in wide and 0.2 in thick. They were loaded with layers of sheet explosive 3/8in wide, cut into diamond shapes, so as to produce a triangular impulsive velocity distribution.

The impulse imparted to the beam depends not only on the weight of explosive but is also influenced by the leader arrangement and attennuator. Therefore calibration tests have been performed [52] to determine the necessary constants. It resulted that for diamond shaped sheet explosive 3/8in wide

$$W_e' = W_e + 0.03564 \quad \text{gm} \tag{6.1}$$

where W_e is the weight of the explosive and, for the present explosive type the specific impulse is:

$$I_s = 0.2265 \quad \text{lb.sec/gm} \tag{6.2}$$

The total impulse imparted to the beam is:

$$I = I_s \; W_e' \tag{6.3}$$

and the peak value of the velocity distribution is

$$V_o = \frac{2\,I}{\rho\; H\; B\; d} \tag{6.4}$$

where d is the length of the beam section which is covered with the explosive.

The ratio between kinetic energy and the maximum amount of strain energy which can be absorbed by a structure in a wholly elastic manner is estimated by:

$$E_r = \frac{\rho\; E\; V_o^2}{3\;\sigma_o^2} \tag{6.5}$$

where $\sigma_o = 49296 \begin{matrix} +563 \\ -1007 \end{matrix}$ lb/in^2.

The energy-absorbing characteristics can be measured by the dimensionless parameter

$$\bar{\gamma} = \frac{W_m}{K_o/(\sigma_o\; H^2)} \tag{6.6}$$

where K_o is the total initial kinetic energy.

The permanent transverse displacements were given by the difference dial gauge readings before and after the test, with the beam still in the clamps. Only the maximum transverse displacements, are shown in Table 1, and are plotted in Figures 8 , 9 and 10, together with results from Jones and Wierzbicki [52].

TEST No.	MODE No.	B (in)	H (in)	2L (in)	W_e (gm)	V_o (in/sec)	$\frac{W_m}{H}$	average W_m/H	λ	avg. λ	E_r	γ
1	1	.5992	.1994	4.9906	.385	1273		.226		5.17	.59	2.19
2	1	.6000	.1993	4.9704	.442	1450		.287		6.66	.76	2.14
3	1	.6000	.1988	4.9553	.525	1711		.483		9.27	1.06	2.58
4	2	.6002	.2000	4.9938	.255	1750	.1205 .2041	.162		9.72	1.11	1.67
5	2	.6000	.1997	4.9955	.331	2211	.3574 .2697	.314		15.58	1.77	2.01
6	3	.5996	.2004	4.9810	.259 .216 .259	2503 2580 2503	-.10798 .20778 -.16379	.159	19.72 20.94 19.72	20.13	2.31	1.21
7	3	.6000	.2002	4.9708	.305 .252 .305	2896 2950 2896	-.2079 .2515 -.2292	.230	26.33 27.32 26.33	26.8	3.23	1.29
8	3	.5996	.2005	4.9750	.261 .219 .261	2518 2608 2518	-.17138 +.27512 -.20944	.219	19.88 21.32 19.88	20.36	2.35	1.07

TABLE 1. EXPERIMENTAL RESULTS

7. DISCUSSION AND CONCLUSIONS

A study into the higher mode dynamic plastic response of beams is reported here. Different solutions methods are used and results are compared with experiments.

It is shown that the inclusion of finite-deflections improves significantly the infinitesimal deflection solutions what agrees with previous results [19-21,25,47,52].

The method developed by Jones [47] to account for the effect of finite-deflections proved simple to use and gave good results. When using the Tresca yield condition, as appropriate for metals, reasonable results were obtained as can be seen in Figures 8 to 10. The use of a cruder description of material behaviour such as the square interaction curve, without strain-rate effects was much simpler to use and gave once more [47,51,52] surprizingly good design estimates of final deflection, equations (3.5), (3.14), (3.18), as shown in Figures 8 to 10.

The numerical procedure reported in section 4 which satisfies the field equations at every time step is more complicated and, for the present problem gave essentially the same results as using the previously mentioned method. It allowed for the hinge to propagate and it was found

that the hinge moved only slightly during the motion and the convergence in the numerical iterative process was very rapid what confirms the observations of Symonds and Chon [42]. However, at each time step the moment was computed throughout the beam and substantial yield violations were found to spread during the motion.

The elastic-plastic numerical analysis is undoutly the most compreensive and complex analysis method used. However, after being incorporated in a computer code, it becomes relatively simple to utilise. As can be seen in Figure 9, it gives reasonable predictions, although with a tendency of overestimating the deflections. This can also be observed in the results reported in [6] where the prediction of the final deflection of an impulsively loaded beam is somewhat higher than the experiment.

It is apparent from the experimental results that, when the initial velocity is arranged with the shape of the mode considered, the beam deforms accordingly. Also, from experiments reported in [52] with uniformly distributed load, it seem that the beams with different loading conditions tend to deform in the mode shapes reported. However, it is still to be known how a beam would deform when subjected to loading conditions substantially different from the mode shape, such as a triangular impulses

with it's peak not coinciding with the maximum deflection of the mode shape.

The use of normal modes is a powerfull tool when analysing the elastic vibrations of linear systems, the only case in which it is exact to use. However, it has been used as an approximation in non-linear cases [65-68]. It rest to be determined if such concepts could be extended to plasticity and the higher dynamic plastic modes used in a modal superposition formulation.

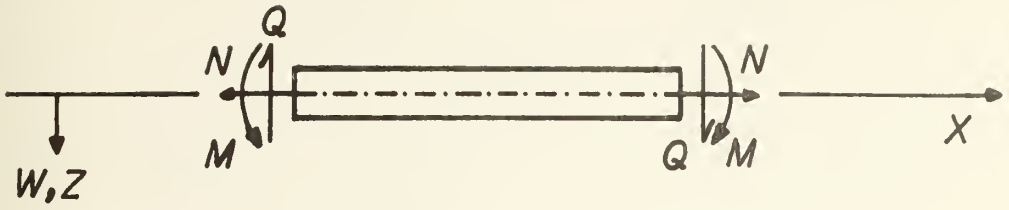

Figure 1. Free body diagram of a beam element showing the positive directions of the indicated quantities. For the case of infinitesimal deflections the axial force N is absent.

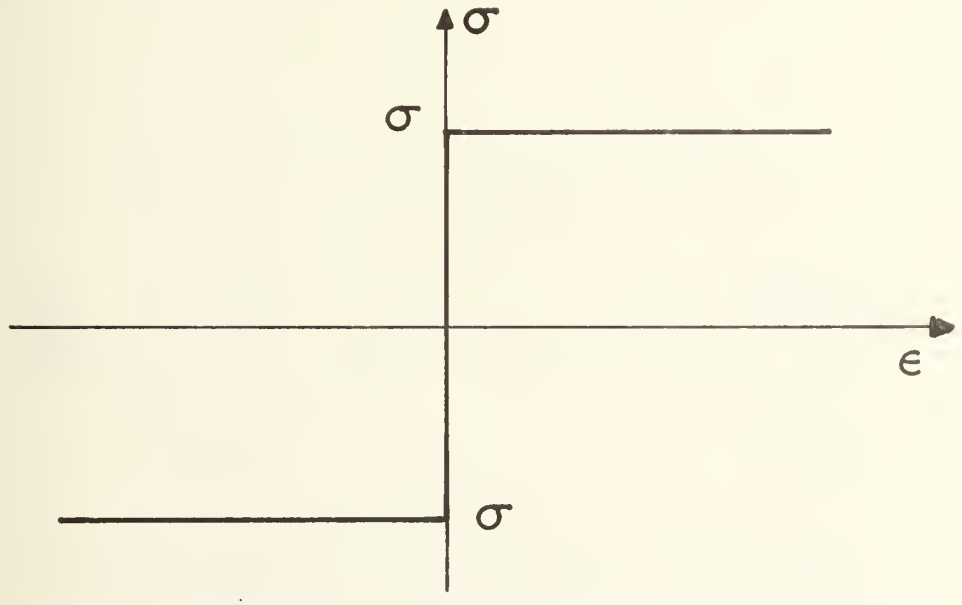

Figure 2. Rigid plastic behaviour.

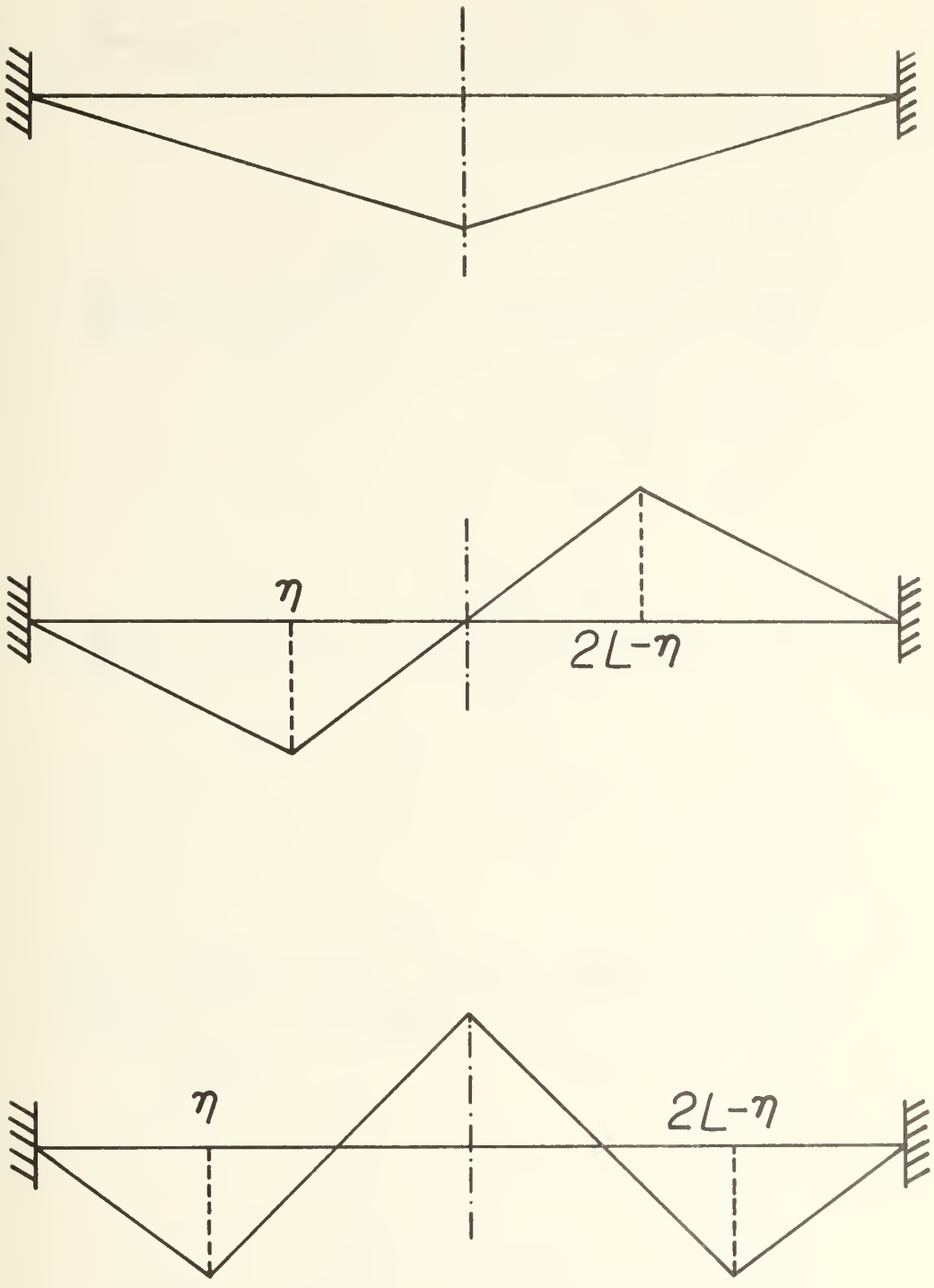

Figure 3. First, Second and Third Mode Shapes

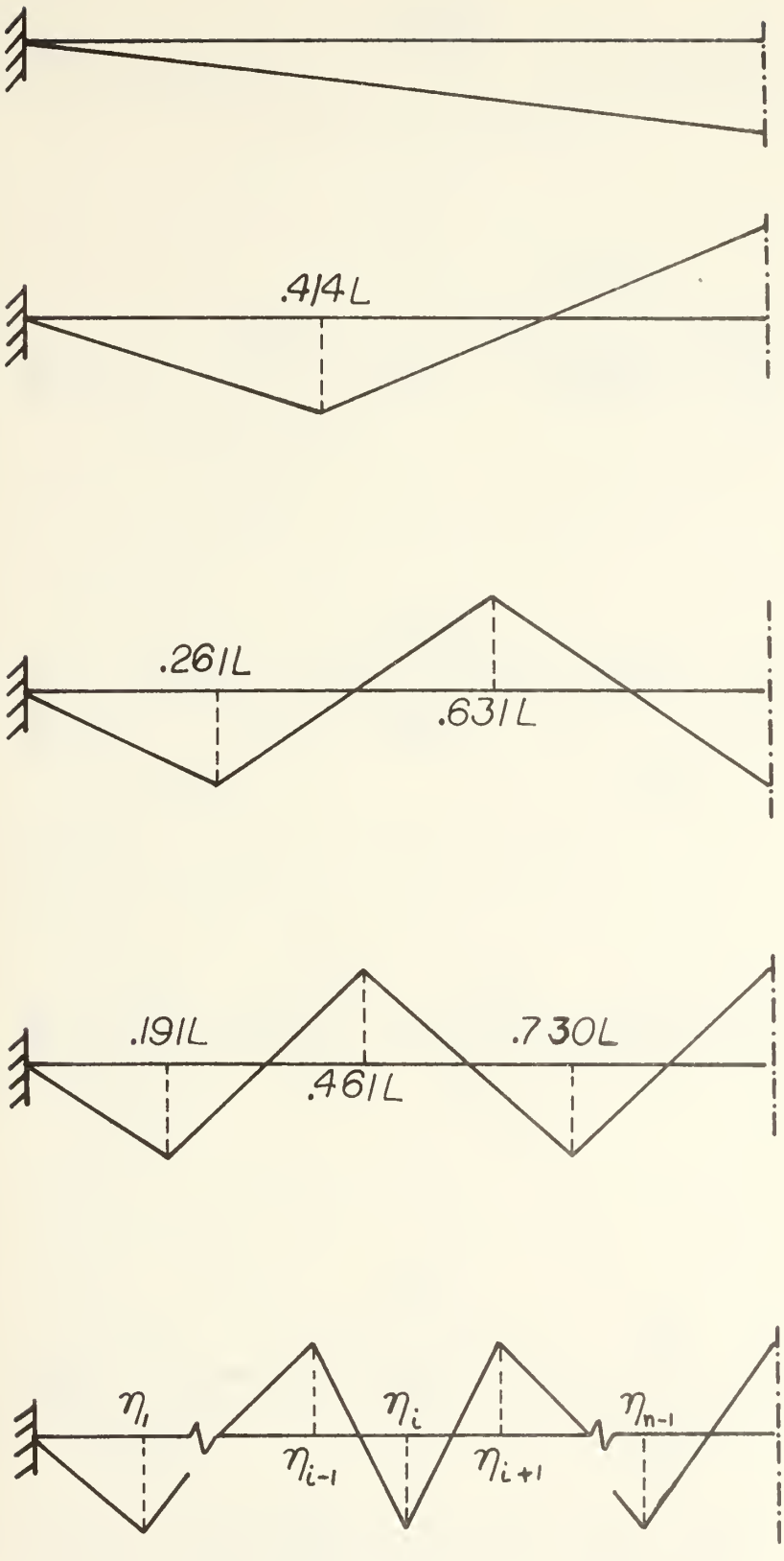

Figure 4. Symmetric Modes: Half Span of the 1^{st}, 3^{rd}, 5^{th}, 7^{th} and i^{th} mode.

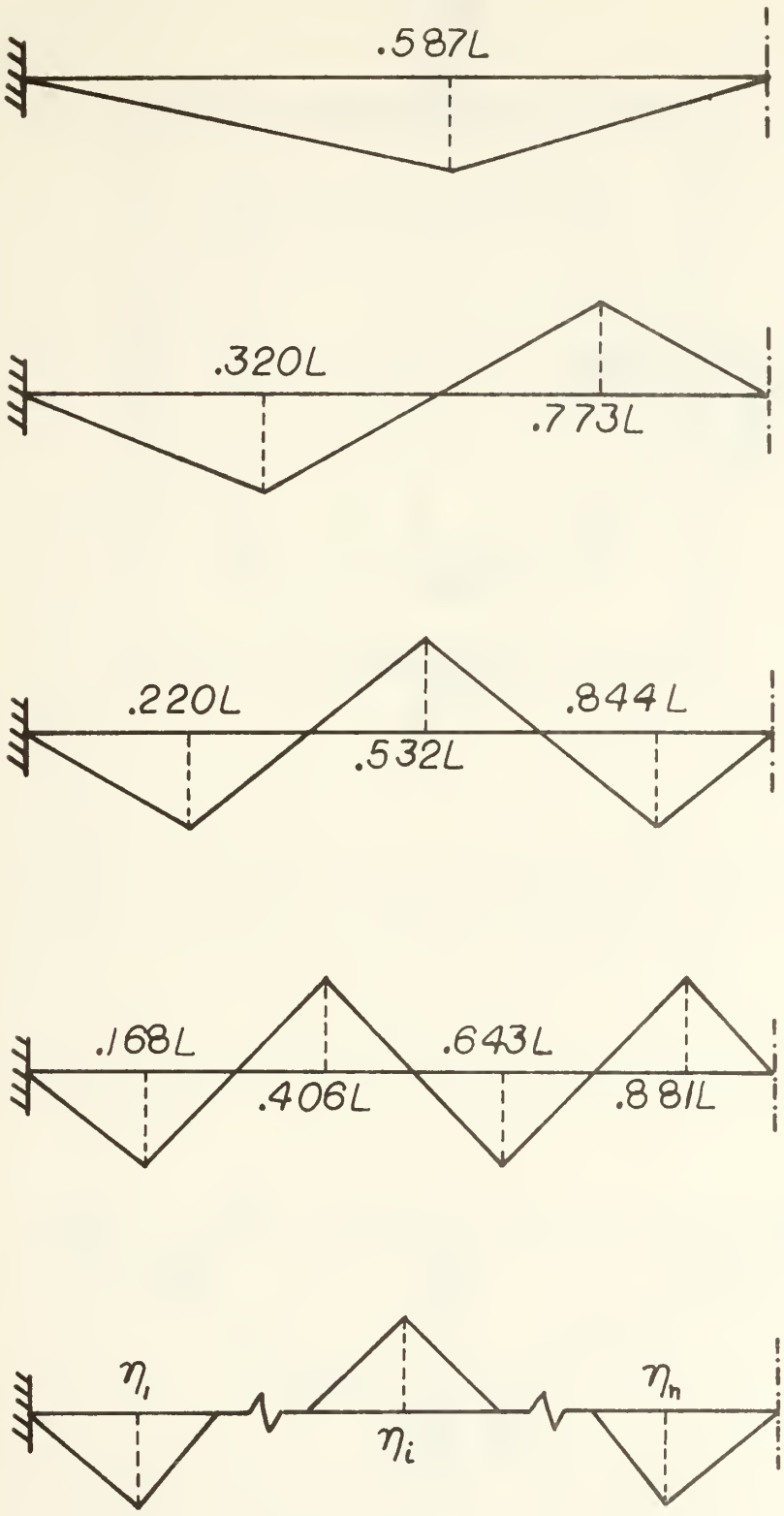

Figure 5. Antisymmetric Modes: Half Span of the $2^{nd}, 4^{th}, 6^{th}, 8^{th}$ and i^{th} mode.

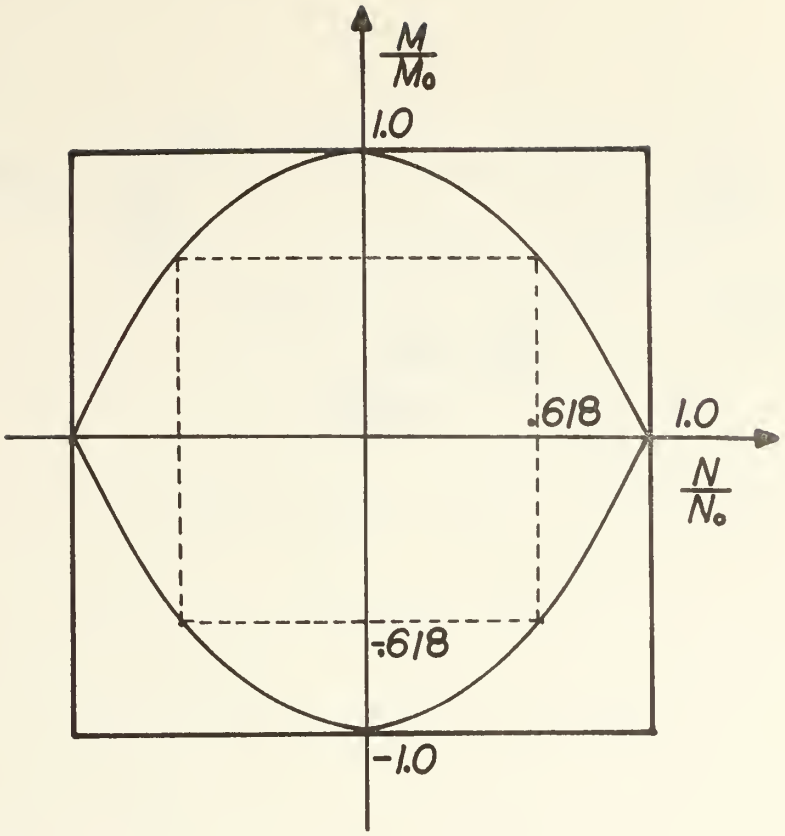

Figure 6. Tresca Yield Condition with the Circunscribing and Inscribing Square Interaction Curve.

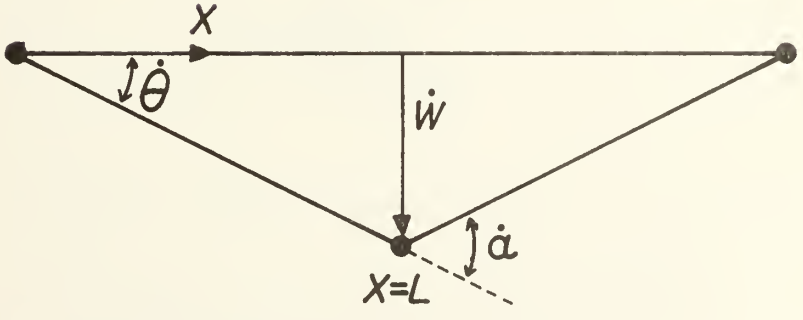

(a) First Mode

Figure 7. Collapse Mechanisms Used in Approximate Procedure.

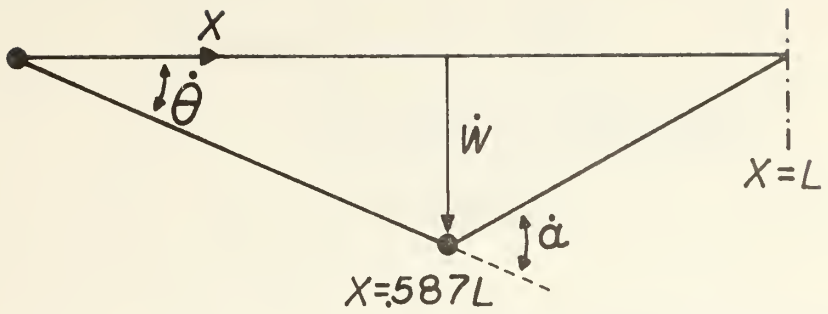

(b) Second Mode (half-span)

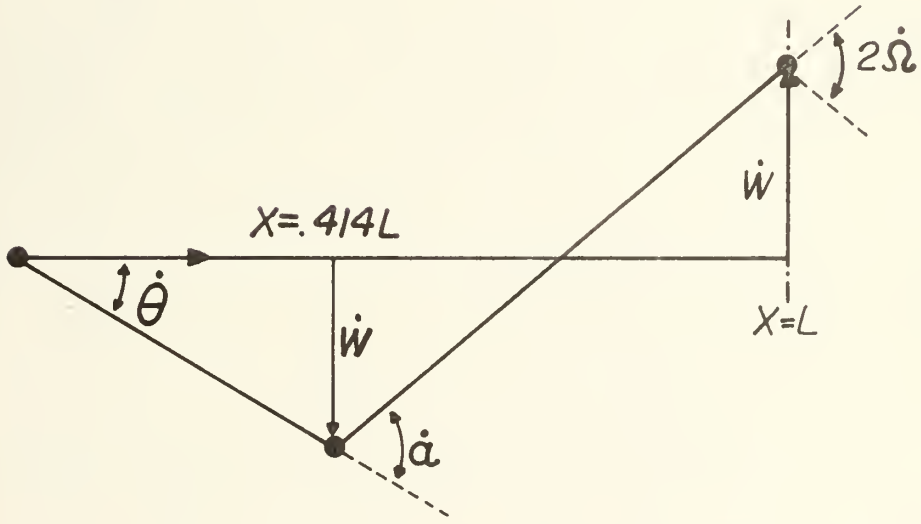

(c) Third Mode (half-span)

Figure 7. Collapse Mechanisms Used in the approximate Procedure

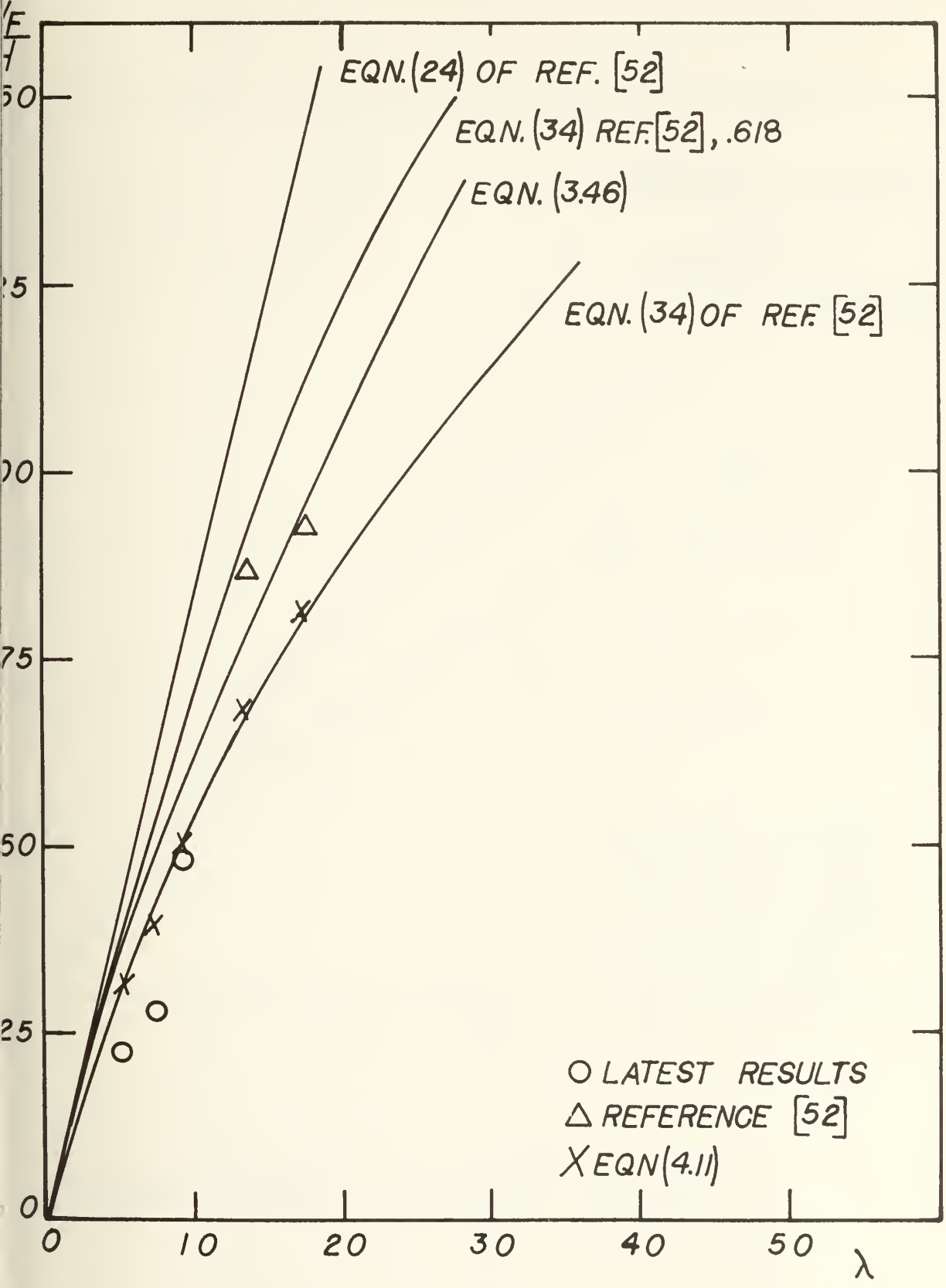

FIGURE N.8 FIRST MODE

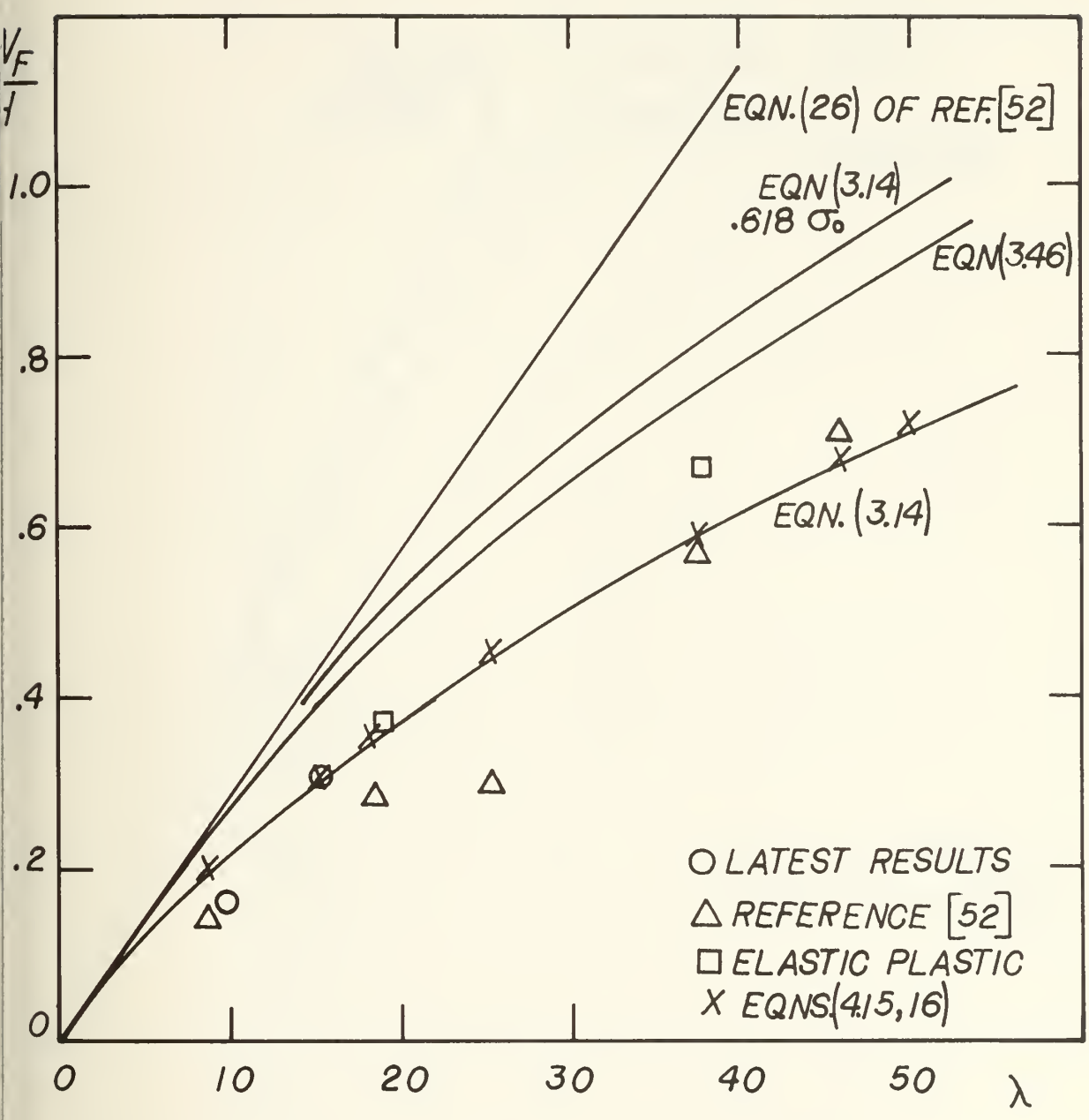

FIGURE N.9 SECOND MODE

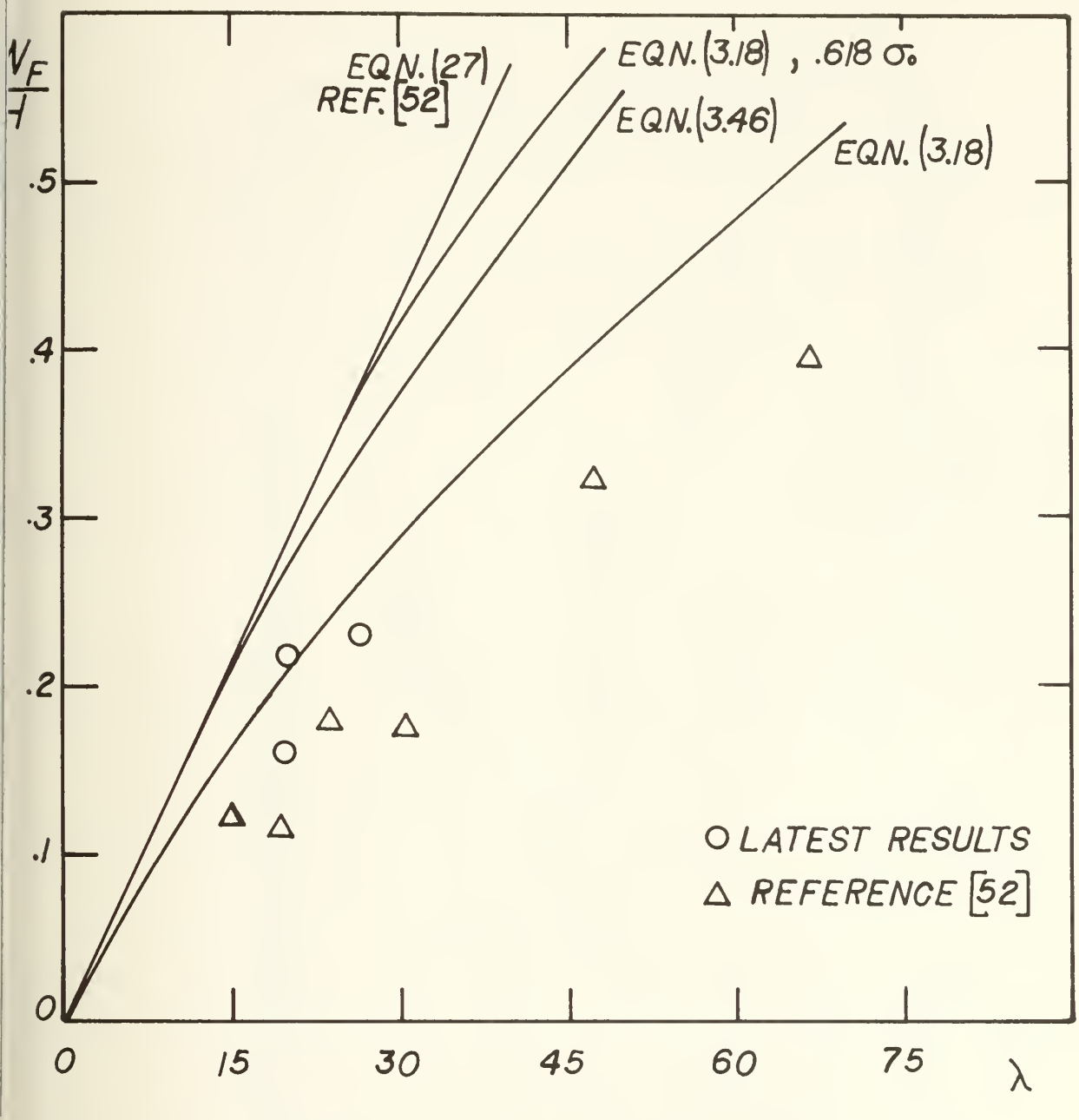

FIGURE No. 10 THIRD MODE

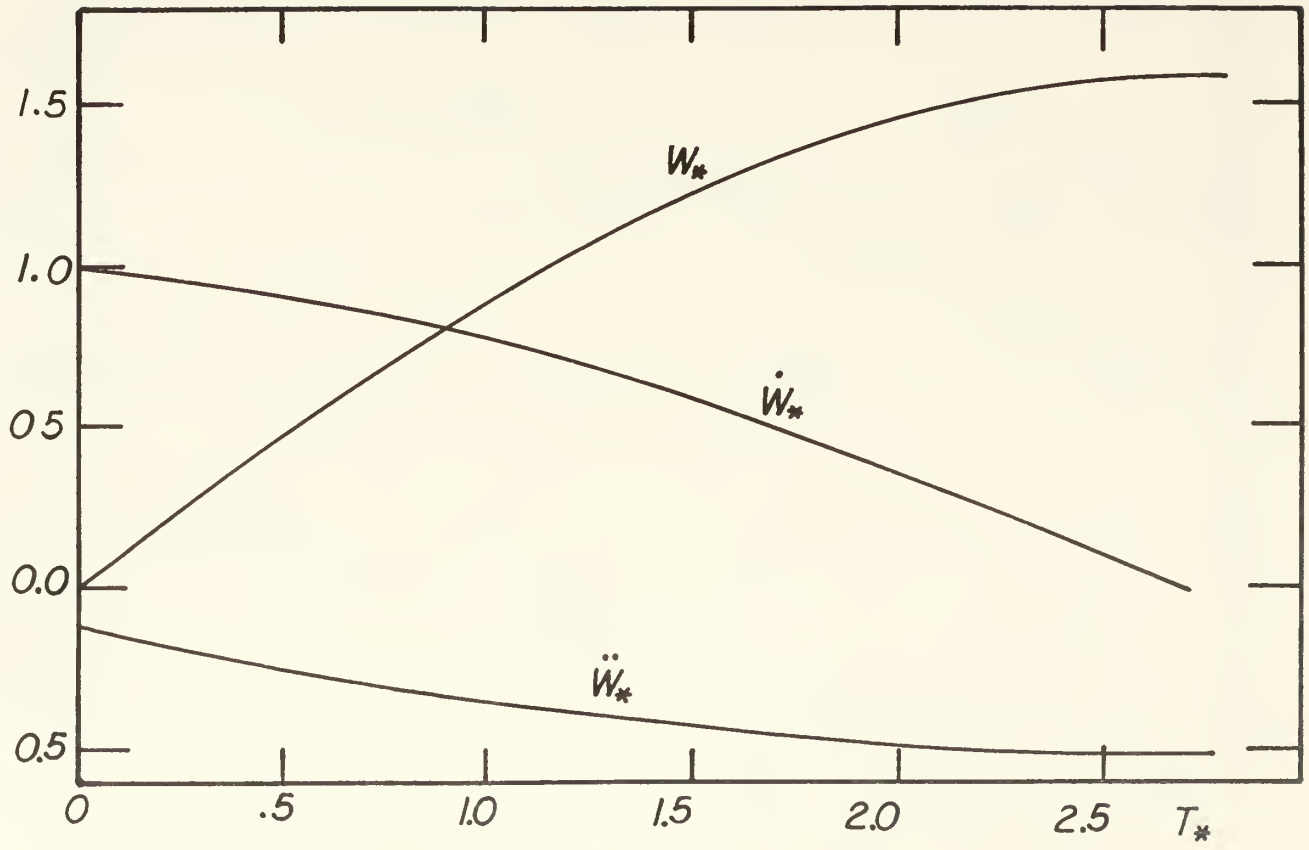

Figure 13. Solution of [illegible], first mode, for [illegible]

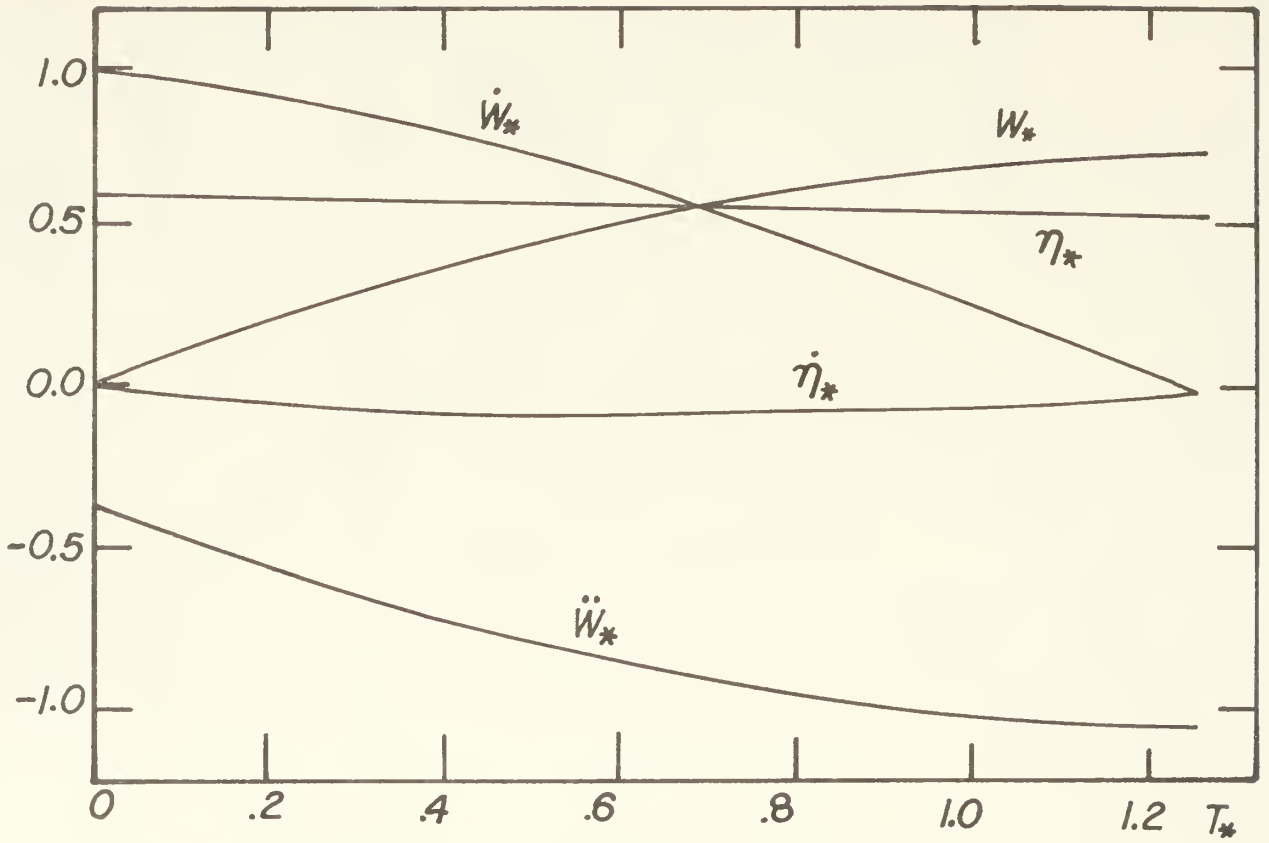

Figure 12, Solution of equations (4.15,16), Second Mode for $\lambda=50$

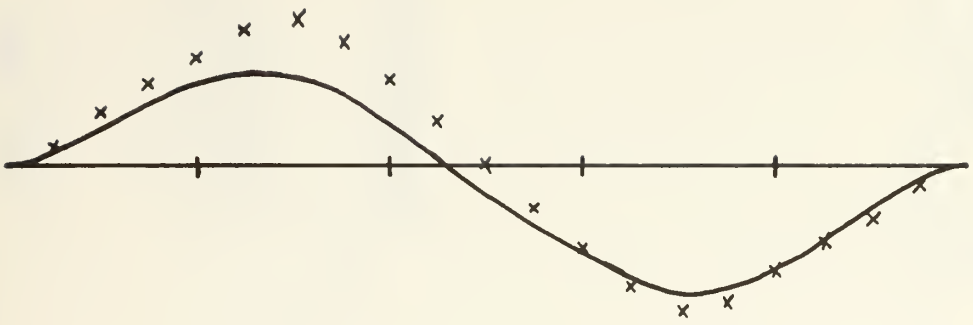

(a) Specimen 9

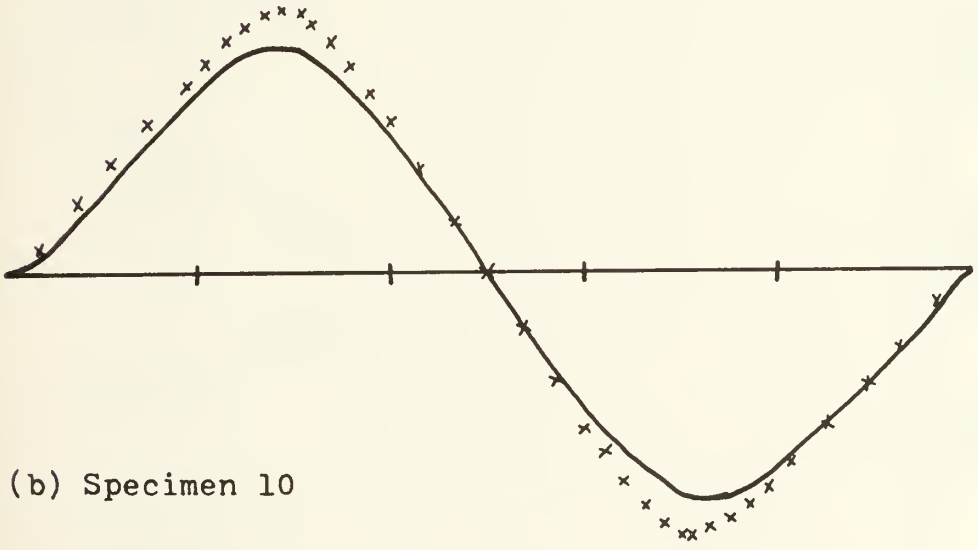

(b) Specimen 10

Figure 13. Deflected Shape of Specimens 9 and 10 of Reference [52] compared with results of Elastic-Plastic Analysis. —— experiment x computed

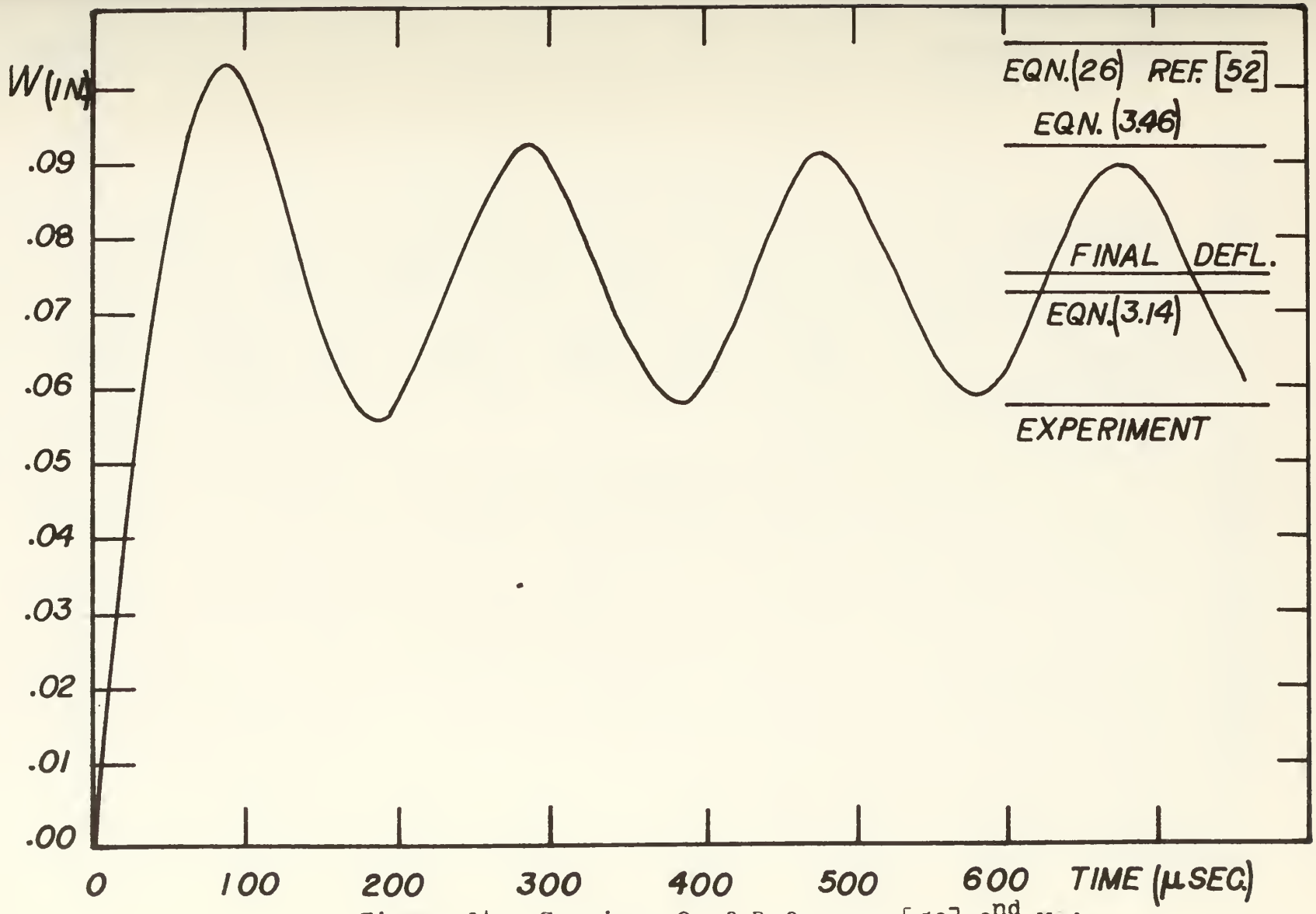

Figure 14 . Specimen 9 of Reference [52]-2nd Mode

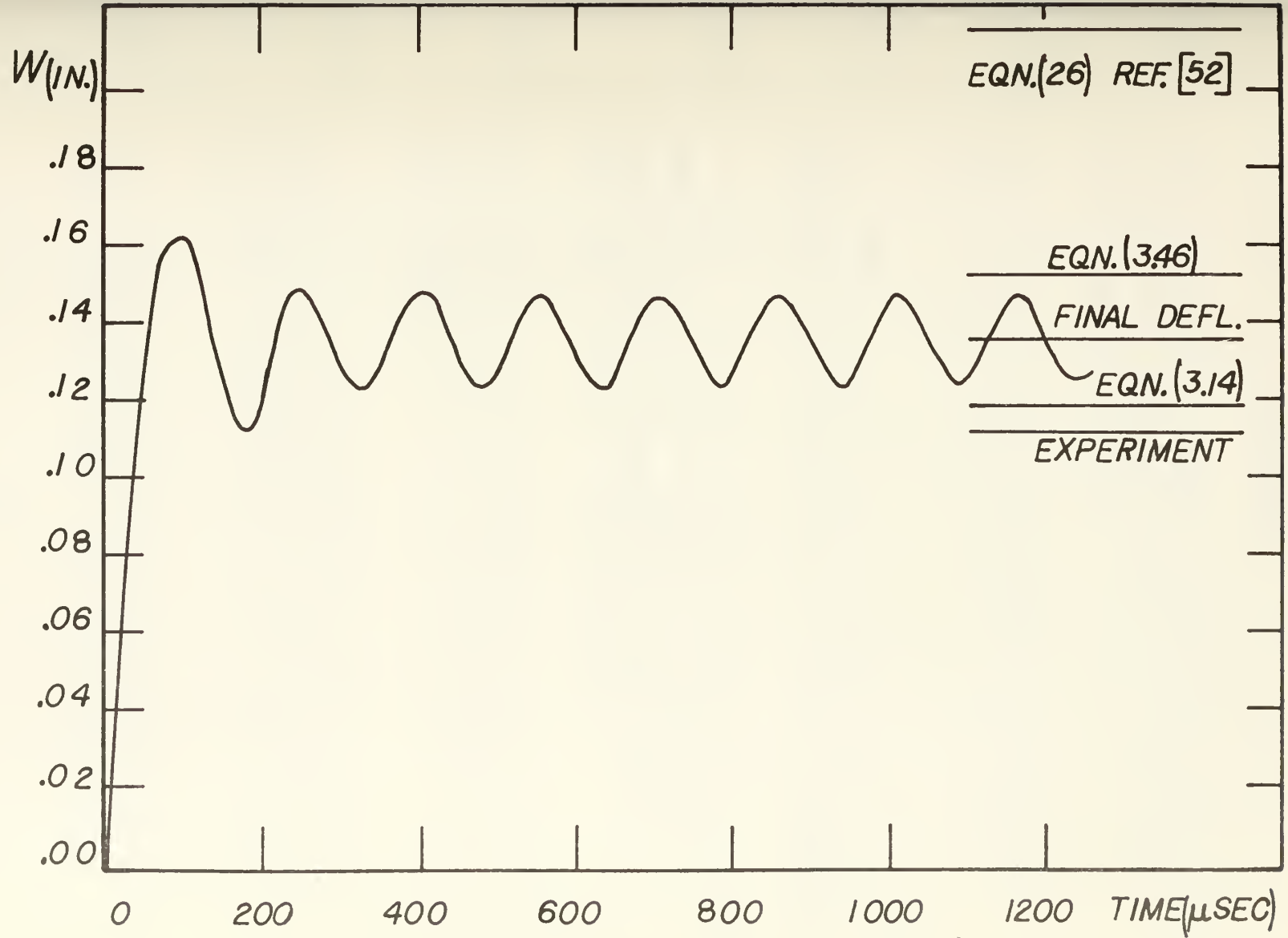

Figure 15. Specimen 10 of reference [52] - 2nd plate

REFERENCES

[1] - E.H. Lee, and P.S. Symonds, "Large Plastic Deformation of Beams under Transverse Impact", J. Appl. Mech., Vol 19, 1952, pp 308-314.

[2] - M.F. Conroy, "Plastic-Rigid Analysis of Long Beams under Transverse Impact Loading", J. Appl. Mech., Vol 19, 1952, pp 465-470.

[3] - E.A. Witmer, H.A. Balmer, J.W. Leech, and T.H.H. Pian, "Large Dynamic Deformations fo Beams, Rings, Plates and Shells", AIAA Journal, Vol 1, 1963, pp 1848-1857.

[4] - L. Morino, J.W. Leech, and E.A. Witmer, "An Improved Numerical Calculation Technique of Large Elastic-Plastic Transient Deformations of Thin Shells", J. Appl. Mech., Vol 38, 1971, pp 423-436.

[5] - H.D. Hibbitt, P.V. Marçal, and J.R. Rice, " A Finite Element Formulation for Problems of Large Strain and Large Displacement", Int. J. Solids Struct., Vol 6, 1970, pp 1069.

[6] - R.W.-H. Wu, and E.A. Witmer, "Non-linear Transient Responses of Structures by the Spacial Finite-Element Method, AIAA Journal, Vol 11, 1973, pp 1110--1117.

[7] - J.H. Argyris, and D.W. Scharpf, "Finite Elements in Time and Space", Nuclear Engineering and Design,

Vol 10, 1969, pp 456-464.

[8] - O.C. Zienkiewicz, and C.J. Parekh, "Transient Field Problems: Two-Dimensional and Three-Dimensional Analysis by Isoparametric Finite Element", Int. J. for Num. Meth. Eng., Vol 2, 1970, pp 61-71.

[9] - P.S. Symonds, "Survey of Methods of Analysis for Plastic Deformation of Structures under Dynamic Loading", Brown University Report BU/NSRDC/1-67,1967.

[10] - S.R. Bodner, and P.S. Symonds, "Experimental and Theoretical Investigation of the Plastic Deformation of Cantilever Beams Subjected to Impulsive Loading", J. Appl. Mech., Vol 29, 1962, pp 719-727.

[11] - P.S. Symonds, "Large Plastic Deformations of Beams under Blast Type Loading", Proc. 2nd U.S. Natl. Cong. Appl. Mech., pp 505-515.

[12] - E.W. Parker, "The Permanent Deformation of a Cantilever Struck Transversly at it's Tip", Proc. Roy. Soc., A, Vol 228, 1955, pp 462-476.

[13] - B. Rawlings, "Dynamic Changes in Mode in Rigid-Plastic Structures", J. Eng. Mech. Div. ASCE, Vol 91, EM2, 1965, pp 1-20.

[14] - H.G. Hopkins, and W. Prager, "On the Dynamics of Plastic Circular Plates", Z. Angew. Math. u Phys., Vol 5, 1954, pp 317

[15] - A.D. Cox, and L.W. Morland, "Dynamic Plastic Deformation of Simply-Supported Square Plates", J. Mech. Phys. Solids, Vol 7, 1959, pp 229-241.

[16] - P.G. Hodge, Jr., "Impact Pressure Loading of Rigid--Plastic Cylindrical Shells", J. Mech. Phys. Solids, Vol 3, 1955, pp 176-188.

[17] - J. S. Humphreys, "Plastic Deformation of Impulsively Loaded Straight Clamped Beams", J. Appl. Mech., Vol 32, 1965, pp 7-10.

[18] - A.L. Florence, and R.D. Firth, "Rigid-Plastic Beams under Uniformly Distributed Impulses", J. Appl. Mech., Vol 32, 1965, pp 481-488.

[19] - P.S. Symonds, and T.J. Mentel, "Impulsive Loading of Plastic Beams with Axial Constraints", J. Mech. Phys. Solids, Vol 6, 1958, pp 186-202.

[20] - T.C.T. Ting, "Large Deformation of a Rigid, Ideally Plastic Cantilever Beam", J. Appl. Mech., Vol 32, 1965, pp 295-302.

[21] - N. Jones, "Finite-Deflections of a Simply-Supported Rigid-Plastic Annular Plate Loaded Dynamically", Int. J. Solids Struct., Vol 4, 1968, pp 593-603.

[22] - T.C.T. Ting, " The Plastic Deformation of a Cantilever Beam with Strain-Rate Sensitivity under Impulsive Loading", J. Appl. Mech., Vol 31, 1964, pp 38-42.

[23] - N. Perrone, "On a Simplified Method for Solving Impulsively Loaded Structures of Rate-Sensitive Materials", J. Appl. Mech., Vol 32, 1965, pp 489-492.

[24] - P.S. Symonds, "Viscoplastic Behaviour in Response of Structures to Dynamic Loading", Behaviour of Materials under Dynamic Loading, N.J.Hunffington, ed, ASME 1965, pp 106-124.

[25] - P.S. Symonds, and N. Jones, "Impulsive Loading of Fully Clamped Beams with Finite Plastic Deflections and Strain-Rate Sensitivity", Int. J. Mech. Sci., Vol 14, 1972, pp 49-69.

[26] - N. Jones, "Influence of Strain-Hardening and Strain--Rate-Sensitivity on the Permanent Deformation of Impulsively Loaded Rigid-Plastic Beams", Int. J. Mech. Sci., Vol 9, 1967, pp 777-796.

[27] - N. Jones, "Finite-Deflections of a Rigid-Viscoplastic Strain-Hardening Annular Plate Loaded Impulsively", J. Appl. Mech., Vol 35, 1968, pp 349-356.

[28] - N. Jones, R.N. Griffin, R.E. Van Duzer, "An Experimental Study into the Dynamic Plastic Behaviour of Wide Beams and Rectangular Plates", Int. J. Mech. Sci., Vol 13. 1971, pp 721-735.

[29] - N. Jones, J.W. Dumas, J.G. Giannotti, and K.E. Grassit, "The Dynamic Plastic Behaviour of Shells", Dynamic Response of Structures, eds. G. Herrmann and

N. Perrone, Pergamon Press, 1972, pp 1-29.

[30] - J.B. Martin, "Impulsive Loading Theorems for Rigid--Plastic Continua", J. Eng. Mech. Div., ASCE, EM5, 1964, pp 27-42.

[31] - W.J. Moralles, and G.E. Nevill, "Lower Bounds on Deformations of Dynamically Loaded Rigid-Plastic Continua", AIAA Journal, Vol 8, 1970, pp 2043-2046.

[32] - T. Wierzbicki, "Bounds on Large Dynamic Deformations of Structures", J. Eng. Mech. Div., ASCE, Vol 96,1970 pp 267.

[33] - J.B. Martin, "Time and Displacement Bound Theorems for Viscous and Rigid-Viscoplastic Continua Subjected to Impulsive Loading", Developments in Theoretical and Applied Mechanics, Vol 3, 1967, pp 1-22.

[34] - P.S. Symonds,and C.T. Chon, "Bounds for Finite Deflections of Impulsively Loaded Structures with Time-Dependent Plastic Behaviour", Int. J. Solids Struct., Vol 11. 1975, pp 403-423.

[35] - J.B. Martin, and P.S. Symonds, "Mode Approximations for impulsively Loaded Rigid-Plastic Structures", J. Eng. Mech. Div., ASCE, Vol 92, 1966, EM5, pp 43.

[36] - J.B. Martin, "A note on the Uniqueness of Solutions for Dynamically Loaded Rigid-Plastic and Rigid-Viscoplastic Continua", J. Appl. Mech., Vol 33, 1966,

pp 207.

[37] - V.P. Tamuzh, "On a Minimum Principle in Dynamic of Rigid-Plastic Bodies",Prik. Mat. i Mekh., Vol 26, 1962, pp 715-722.

[38] - L.S.S. Lee, and J.B. Martin, "Approximate Solutions of Impulsively Loaded Structures of a Rate Sensitive Material", Z. Angew. Math. u Phys., Vol 21, 1970, pp 1011-1032.

[39] - L.S.S. Lee, "Mode Response of Dynamically Loaded Structures", J. Appl. Mech., Vol 39, 1972, pp 904.

[40] - H.-S. Ho, "Convergent Approximation of Problems of Impulsively Loaded Structures", J. Appl. Mech., Vol 38, 1971, pp 852-860.

[41] - D.C. Drucker, W. Prager, and H.G. Greenberg, "Extended Limit Design Theorem for Continuous Media", Quart. Appl. Math., Vol 9, 1952, pp 381-389.

[42] - P.S. Symonds, and C.T. Chon, "Approximation Techniques of Impulsive Loading of Structures of Time-Dependent Plastic Behaviour with Finite Deflections", Proc. Conf. in Mech. Prop. Mat. at High Strain-Rates, Inst. of Phys., London, 1974.

[43] - P.S. Symonds, and T. Wierzbicki, "On an Extremum Principle for Mode Form Solutions in Plastic Structural Dynamics", J. Appl. Mech., Vol 42, 1975, pp 630-640.

[44] - T. Wierzbicki, "Direct Variational Approach to Dynamic Plastic Mode Solutions", Bull. Acad. Pol. Sci., Ser. Sci., Tech., Vol 23, 1975, pp 299.

[45] - A. Sawczuk, "On Initiation of the Membrane Action in Rigid-Plastic Plates", J. Méc., Vol 3, 1964, pp 15-23.

[46] - A. Sawczuk, "Large-Deflections of Rigid-Plastic Plates", Proc. 11th Int. Cong. Appl. Mech., 1964, pp 224-228.

[47] - N. Jones, "A Theoretical Study of the Dynamic Plastic Behaviour of Beams and Plates with Finite-Deflections", Int. J. Solids Struct., Vol 7, 1971, pp 1007-1029.

[48] - R.M. Walters, and N. Jones, "An Approximate Theoretical Study on the Dynamic Plastic Behaviour of Shells", Int. J. Non-Linear Mech., Vol 7, 1972, pp 255-273.

[49] - N. Jones, T.O. Uran, S.A. Tekin, "The Dynamic Plastic Behaviour of Fully Clamped Rectangular Plates", Int. J. Solids Struct., Vol 6, 1970, pp 1499-1512.

[50] - N. Jones, R.A. Baeder, "An Experimental Study of the Dynamic Plastic Behaviour of Rectangular Plates", Symp. on Plastic Analysis of Structures, Min. of Educ., Poly. Int. Jassy, Civ. Eng. Fac. Rumania, Vol 1, 1972, pp 476-497.

[51] - N. Jones, "Plastic Failure of Ductile Beams Loaded

Dynamically, J. Eng. Ind., Feb. 1976.

[52] - N. Jones,and T. Wierzbicki, "A Study of the Higher Modal Dynamic Plastic Response of Beams", M.I.T. Department of Ocean Engineering Report 76-3, 1976.

[53] - N. Jones, "Influence of In-plane Displacements at the Boundaries of Rigid-Plastic Beams and Plates", Int. J. Mech. Sci., Vol 15, 1973, pp 547-561.

[54] - P. S. Symonds, "Plastic Shear Deformations in Dynamic Load Problems", Engineering Plasticity, eds. Heyman and Leckie, 1968, pp 647-664, Cambridge University Press.

[55] - K.W.Johanssen, "Yield-Line Theory", Cement and Concrete Assoc., London 1962.

[56] - N. Jones, "Review of the Plastic Behaviour of Beams and Plates", Int. Shipbuilding Prog., Vol 19, 1972, pp 313-327.

[57] - N. Jones, "Consistent Equations fot the Large Deflections of Structures", Bull. Mech. Eng. Educ., Vol 10, 1971, pp 9-20

[58] - M. Geradin, "A Classification and Discussion of Integration Operators for Transient Structural Response", AIAA Paper Nº. 74-105, AIAA 12th Aerospace Sciences Meeting, 1974.

[59] - R.E. Nickell, "On the Stability of Approximation Ope-

rators in Problems of Structural Dynamics", Int. J. Solids Struct., Vol 7, 1971, pp 301-319.

[60] - K.C. Park, "An Improved Stiffly Stable Method for Direct Integration of Non-linear Structural Dynamic Equations, J. Appl. Mech., Vol , 1975, pp 464-470.

[61] - K.C. Park, "Practical Aspects of Numerical Time Integration", 2nd Nat. Symp. on Computerized Structural Analysis and Design, 1976, to be published in Int.J. Computers and Structures.

[62] - N.M. Newmark, " A Method of Computation for Structural Dynamics", J. Eng. Mech. Div. ASCE, Vol 85, 1959, EM3, pp 67-94.

[63] - T.J.R. Hudges, "Stability,Convergence and Growth and Decay of Energy of the Average Acceleration Method in Non-linear Structural Dynamics", 2nd Nat. Symp. on Compuerized Structural Analysis and Design, 1976, to be published in Int. J. Computers and Structures.

[64] - R.W.-H. Wu, and E.A. Witmer, "Computer Program - JET 3 to calculate the Large Elastic Plastic Dynamically--Induced Deformations of Free and Restrained, Partial and/or Complete Structural Rings", NASA CR-120993, 1972.

[65] - R.S. Dunham, R.E. Nickell, and D.C. Stickler, "Integration Operators for Transient Structural Response", Int. J. Computers and Structures, Vol 2,1972, pp 1-15.

[66] - K. T. Kavanagh, "An Approximate Algorith for the Reanalysis of Structures by the Finite-Element Method", Int. J. Computers and Structures, Vol 2, 1972, pp 713-722.

[67] - R.E. Nickell, "Non-Linear Dynamics by Mode Superposition", AIAA/ASME/SAE 15th Structures, Structural Dynamics and Materials Conference, 1974.

[68] - N.F. Morris, "The use of Modal Superposition in Non-Linear Dynamics", 2nd Nat. Symp. on Computerized Structural Analysis and Design, 1976, to be published in Int. J. Computers and Structures.

APPENDIX

Contains the results of the analysis described in section 4 together with the listing of the computer programs used:

Results for First Mode from Equation (4.11)

Results for Second Mode from Equations (4.15,16)

Program Listing: First Mode, Limited Interaction

Program Listing: Seconde Mode, Limited Interaction

λ	W_{*f}	t_{*f}	Δt	Time step	Iter.	Yield Viol. Zone	Max. M/M_o	Max. M at x/L
5.17	.3251	.602	.010 .0025	69	2 1	.71-1.29	1.09	.85
6.66	.3972	.727	.010 .0025	83	2 1	.67-1.33	1.12	.83
9.27	.5112	.925	.010 .0025	105	2 1	.62-1.38	1.18	.83
13.74	.6811	1.212	.010 .0025	136	2 1	.55-1.45	1.28	.79
17.70	.8134	1.432	.010 .0025	160	2 1	.53-1.47	1.36	.76
50.00	1.6015	2.715	.050 .0025	80	2 1	.36-1.64	1.90	.70

TABLE 2. Results for First Mode from Equation (4.1)

λ	W_{*f}	$*f$	t_{*t}	Δt	Time Step	Iter.	Sub Iter.	Yield Viol. Zone	Max. M/M_o	Max. M at x/L
9.4	.2080	.5542	.389	.005 .002	83	2 1	3 2	0.44-0.69	1.07	0.62
15.50	.3091	.5461	.567	.005 .002	121	2 1	3 2	0.41-0.73	1.12	0.65
[illegible]	[illegible]	[illegible]	[illegible]	.01 .002	73	2 1	3 2	0.38-0.75	1.15	0.65
25.57	.4489	.5382	.804	.01 .002	92	2 1	3 2	.35-.77	1.21	0.65
37.84	.5920	.5325	.042	.01 .002	119	2 1	3 2	0.3[illegible]-.79	1.30	0.66
45.99	.6762	.5299	1.182	.025 .002	64	2 1	4 3	0.29-.81	1.36	.66
50.00	.7152	.5288	1.246	.025 .002	73	2 1	4 3	.29-.81	1.39	.67

TABLE 3. Results for Second Mode from equations (4.15, 4.16)

```
C FIRST MODE, LIMITED INTERACTION

      DIMENSION B(200),BD(200),BDD(200),H(200),T(200),A(200),BB(200)
      DIMENSION IT(200)
      DIMENSION F(21)
      REAL MM(21)

C DEFINE CONSTANTS

      IW=5
      RLAM=50.
      DO 11 I=1,200
   11 H(I)=0.01
      NREF=5

C DEFINE INITIAL CONDITIONS

      N=1
      T(1)=0.0
      B(1)=0.0
      BD(1)=1.0
      BDD(1)=-6./RLAM

C PERFORM THE CALCULATIONS IN TIME STEPS

      WRITE(IW,105)
      WRITE(IW,115) RLAM
  105 FORMAT (' **********  FIRST MODE, LIMITED INTERACTION *****'//)
  115 FORMAT(1X,'**********LAMDA=',F7.2,'**********'/////)
    1 CONTINUE
      N=N+1
      NN=N-1
C DEFINE THE CONSTANTS FOR EACH TIME STEP
      T(N)=T(NN)+H(N)
      A(NN)=BD(NN)+BDD(NN)*H(N)/2.
      BB(NN)=B(NN)+BD(NN)*H(N)/2.
      IT(N)=0
      B(N)=B(NN)
C INITIATE ITERATION
      ITT=0
    5 IT(N)=IT(N)+1
      ITT=ITT+1
      DD=B(N)
      BDD(N)=-6.*(1.+2.*B(N))/RLAM
      BD(N)=A(NN)+BDD(N)*H(N)/2.
      B(N)=BB(NN)+BD(N)*H(N)/2.
      IF (ITT .GT. 5) GO TO 1
```

```
      ERR=DD-B(N)
      IF (ABS(ERR) .GT. 0.0001) GO TO 5
      M=N
      IF (N .EQ. NREF) GO TO 80
   81 CONTINUE
      IF (N .EQ. 200) GO TO 50
      IF (BD(N) .LT. 0.05) GO TO 45
      GO TO 1
   45 IF (BD(N) .LT. 0.0001 ) GO TO 50
      H(N+1)=0.0025
      GO TO 1

C  CALCULATE THE MOMENT AT DISCRETE POINTS ALONG THE BEAM

   80 NREF=NREF+5
C  DEFINE THE POINTS TO BE CONSIDERED IN MOMENT CALCULATION
      FR=1./20.
      F(1)=0.
      DO 2 I=2,21
    2 F(I)=F(I-1)+FR
C  CALCULATE THE MOMENT
      DO 40 I=1,21
      MM(I)=-RLAM*BDD(N)*(F(I)**2.-1.)*F(I)/6.+1.-2.*F(I)
   40 CONTINUE
      WRITE(IW,110) N
      WRITE(IW,100)  (F(I), I=1,21)
      WRITE(IW,101)  (MM(I), I=1,21)
  100 FORMAT (1X,21F6.2)
  101 FORMAT (1X,21F6.2/)
  110 FORMAT (1X,'******N=',I3,'******')
      GO TO 81

C  MOTION FINISHED.  PRINT THE RESULTS
   50 WRITE(IW,61)
   61 FORMAT ('1')
      WRITE(IW,105)
      WRITE(IW,115) RLAM
      WRITE(IW,55)
   55 FORMAT (2X,'TIME',9X,'DISPL',11X,'VEL',11X,'ACCEL',5X,'IT',5X,'STE
     CP',5X,'DELT')
      DO 56 N=1,M
   56 WRITE(IW,60) T(N),B(N),BD(N),BDD(N),IT(N),N,H(N)
   60 FORMAT (F6.3,3F15.5,5X,I2,5X,I3,5X,F6.4)
      END
```

```
 SECOND MODE, LIMITED INTERACTION

   DIMENSION B(200),BD(200),BDD(200),E(200),ED(200),H(200)
   DIMENSION A(200),BB(200),C(200),IT(200),IST(200),T(200)
   DIMENSION F(50),FF(50)
   REAL M1(50),M2(50)

 DEFINE CONSTANTS
   IW=5
   RLAM=50.
   DO 11 I=1,200
11 H(I)=0.005
   NREF=5

 DEFINE INITIAL CONDITIONS

   N=1
   T(1)=0.
   B(1)=0.
   BD(1)=1.
   E(1)=.5857864376
   BDD(1)=-3.*(2.-E(N))/(RLAM*E(1)*(1.-E(1)))
   ED(1)=6./(RLAM*E(1))+E(1)*BDD(1)

 CALCULATE TIME STEPS

   WRITE(IW,105)
   WRITE(IW,115) RLAM
 1 CONTINUE
   N=N+1
   NN=N-1
 DEFINE CONSTANTS FOR EACH TIME STEP
   T(N)=T(NN)+H(N)
   A(NN)=BD(NN)+BDD(NN)*H(N)/2.
   BB(NN)=B(NN)+BD(NN)*H(N)/2.
   C(NN)=E(NN)+ED(NN)*H(N)/2.
   IT(N)=0
   IST(N)=0
   B(N)=B(NN)
   E(N)=E(NN)
   BDD(N)=BDD(NN)
 INITIATE ITERATION
   ITT=0
 5 IT(N)=IT(N)+1
   ITT=ITT+1
   DD=B(N)
   BD(N)=A(NN)+BDD(N)*H(N)/2.
   B(N)=BB(NN)+BD(N)*H(N)/2.
   IF (ITT .GT. 5) GO TO 1
```

```
C   BEGIN SUBITERATION
      INN=0
   15 IST(N)=IST(N)+1
      INN=INN+1
      D=E(N)
      DB=BDD(N)
      ED(N)=6.*(1.+2.*B(N))/(E(N)*BD(N)*RLAM)+E(N)*BDD(N)/BD(N)
      E(N)=C(NN)+ED(N)*H(N)/2.
      BDD(N)=-3.*(2.-E(N)+4.*B(N))/(RLAM*E(N)*(1.-E(N)))
      IF (INN .GT.10) GO TO 5
      ERROR=D-E(N)
      IF (ABS(ERROR) .GT. 0.0001)  GO TO 15
      ERRO=DB-BDD(N)
      IF (ABS(ERRO) .GT. 0.0001) GO TO 15
C   SUBITERATIONS FINISHED.  GO TO NEXT ITERATION
      ERR=DD-B(N)
      IF (ABS(ERR) .GT. 0.0001) GO TO 5
      M=N
      IF (N .EQ. NREF) GO TO 80
   81 CONTINUE
      IF (N .EQ. 200) GO TO 50
      IF (BD(N) .LT. 0.05) GO TO 45
      GO TO 1
   45 IF (BD(N) .LT. 0.0001 ) GO TO 50
      H(N+1)=0.002
      GO TO 1
   80 NREF=NREF+5
C   CALCULATE THE MOMENT AT DISCRETE POINTS ALONG THE BEAM
C
C   DEFINE THE POINTS TO BE CONSIDERED
      FR=E(N)/20.
      F(1)=0.
      DO 2 I=2,21
    2 F(I)=F(I-1)+FR
      FF(1)=E(N)
      FFR=(1.-E(N))/20.
      DO 3 I=2,21
    3 FF(I)=FF(I-1)+FFR
C   CALCULATE THE MOMENT
      DO 70 I=1,21
        M1(I)=(1.-2.*F(I)/E(N))-RLAM*(BDD(N)-BD(N)*ED(N)/E(N))*(F(I)**
     C3.0-F(I)*E(N)**2.0)/(6.*E(N))
      AM1=1.+E(N)-E(N)*E(N)/2.
      AM2=FF(I)**3.-3.*FF(I)**2.+2.*FF(I)*AM1+E(N)**2.-2.*E(N)
      AM3=BDD(N)+BD(N)*ED(N)/(1.-E(N))
      M2(I)=-(1.-FF(I))/(1.-E(N))+RLAM*AM3*AM2/(6.*(1.-E(N)))
   70 CONTINUE
      WRITE(IW,110) N
      WRITE(IW,100)     (F(I), I=1,21)
      WRITE(IW,100)     (M1(I), I=1,21)
```

```
      WRITE(IW,100)    (FF(I), I=1,21)
      WRITE(IW,101)     (M2(I), I=1,21)
  100 FORMAT (1X,21F6.2)
  101 FORMAT (1X,21F6.2/)
  105 FORMAT (' ********** SECOND MODE, LIMITED INTERACTION ******'//)
  110 FORMAT (1X,'******N=',I3,'******')
  115 FORMAT(1X,'**********LAMDA=',F7.2,'**********'/////)
      GO TO 81
C   MOTION FINISHED.  PRINT THE RESULTS
   50 WRITE(IW,61)
   61 FORMAT ('1')
      WRITE(IW,105)
      WRITE(IW,115) RLAM
      WRITE(IW,55)
   55 FORMAT (2X,'TIME',9X,'HINGE',10X,'DISPL',11X,'VEL',11X,'ACCEL',9X,
     C'HINGEVEL',5X,'IT',5X,'SI',5X,'STEP',5X,'DEL T')
      DO 56 N=1,M
   56 WRITE(IW,60) T(N),E(N),B(N),BD(N),BDD(N),ED(N),IT(N),IST(N),N,H(N
     C)
   60 FORMAT (F6.3,5F15.5,7X,I2,5X,I2,5X,I4,5X,F6.4)
      END
```

Thesis
S6637 Soares
Higher mode dynamic plastic response of beams with finite-deflections.

165501